A neurotrophin functioning with a Toll regulates structural plasticity in a dopaminergic circuit

Jun Sun[1], Francisca Rojo-Cortés[1], Suzana Ulian-Benitez[1,2], Manuel G. Forero[3], Guiyi Li[1], Deepanshu Singh[1], Xiaocui Wang[1], Sebastian Cachero[4], Marta Moreira[1], Dean Kavanagh[5], Gregory Jefferis[4], Vincent Croset[6], and Alicia Hidalgo[1*]

1, Structural Plasticity & Regeneration Lab, Birmingham Centre for Neurogenetics, University of Birmingham, UK;

2, Current address: Buck Institute for Research on Aging, California, US;

3, Semillero Lún, Grupo D+Tec, Universidad de Ibagué, Colombia;

4, MRC LMB, Cambridge, UK;

5, Institute of Biomedical Research, University of Birmingham, UK.

6, Department of Biosciences, Durham University, UK.

*Author for correspondence:

00 44 (0)121 4145416

a.hidalgo@bham.ac.uk

Keywords: Drosophila, structural plasticity, cell survival, synaptogenesis, neurodegeneration, DNT-2, Toll-6, Kek-6, Toll-Like Receptor, Kekkon, Kek.

ABSTRACT

Experience shapes the brain, as neural circuits can be modified by neural stimulation or the lack of it. The molecular mechanisms underlying structural circuit plasticity and how plasticity modifies behaviour, are poorly understood. Subjective experience requires dopamine, a neuromodulator that assigns a value to stimuli, and it also controls behaviour, including locomotion, learning and memory. In *Drosophila*, Toll receptors are ideally placed to translate experience into structural brain change. *Toll-6* is expressed in dopaminergic neurons (DANs), raising the intriguing possibility that Toll-6 could regulate structural plasticity in dopaminergic circuits. *Drosophila* neurotrophin-2 (DNT-2) is the ligand for Toll-6, but whether it is required for circuit structural plasticity was unknown. Here, we show that *DNT-2* expressing neurons connect with DANs, and they modulate each other. Loss of function for *DNT-2* or its receptors *Toll-6* and kinase-less Trk-like *kek-6* caused DAN and synapse loss, impaired dendrite growth and connectivity, decreased synaptic sites and caused locomotion deficits. By contrast, over-expressed *DNT-2* increased dendrite complexity and promoted synaptogenesis. Neuronal activity increased synaptogenesis in DNT-2 and DANs, and over-expression of DNT-2 could mimic this effect. Altering the levels of DNT-2 or Toll-6 could also modify dopamine-dependent behaviours, including locomotion and long-term memory. We conclude that an activity-dependent feedback loop involving dopamine and DNT-2 labelled the circuits engaged, and DNT-2 with Toll-6 and Kek-6 induced structural plasticity in this circuit, modifying brain function.

53

54 **INTRODUCTION**

55 The brain can change throughout life, as new cells are formed or eliminated, axonal and dendritic arbours
56 can grow or shrink, synapses can form or be eliminated(Wiesel 1982, Feldman and Brecht 2005, Holtmaat
57 and Svoboda 2009, Gage 2019). Such changes can be driven by experience, that is, neuronal activity or the
58 lack of it(Wiesel 1982, Maguire et al. 2000, Cotman and Berchtold 2002, Feldman and Brecht 2005, Sur and
59 Rubenstein 2005, Holtmaat and Svoboda 2009, Woollett and Maguire 2011, Chen, CC and Brumberg 2021,
60 Bharmauria et al. 2022). Structural changes result in remodelling of connectivity patterns, and these bring
61 about modifications of behaviour. These can be adaptive, dysfunctional or simply the consequence of
62 opportunistic connections between neurons(Kuner and Flor 2016, Leemhuis et al. 2019, Yang et al. 2020). It
63 is critical to understand how structural modifications to cells influence brain function. This requires linking
64 with cellular resolution molecular mechanisms, neural circuits and resulting behaviours.

65 In the mammalian brain, the neurotrophins (NTs: BDNF, NGF, NT3, NT4) are growth factors
66 underlying structural brain plasticity(Poo 2001, Lu et al. 2005, Park and Poo 2013). They promote neuronal
67 survival, connectivity, neurite growth, synaptogenesis, synaptic plasticity and Long-Term Potentiation (LTP),
68 via their Trk and $p75^{NTR}$ receptors(Poo 2001, Lu et al. 2005, Park and Poo 2013). In fact, all anti-depressants
69 function by stimulating production of BDNF and signalling via its receptor TrkB, leading to increased brain
70 plasticity(Casarotto et al. 2021, Castren and Monteggia 2021). Importantly, NTs have dual functions and can
71 also induce neuronal apoptosis, neurite loss, synapse retraction and Long-Term Depression (LTD), via
72 $p75^{NTR}$ and Sortilin(Lu et al. 2005). Remarkably, these latter functions are shared with neuroinflammation,
73 which in mammals involves Toll-Like Receptors (TLRs)(Squillace and Salvemini 2022). TLRs and Tolls have
74 universal functions in innate immunity across the animals (Gay and Gangloff 2007), and consistently with
75 this, TLRs in the CNS are mostly studied in microglia. However, mammalian *TLRs* are expressed in all CNS
76 cell types, where they can promote not only neuroinflammation, but also neurogenesis, neurite growth and
77 synaptogenesis and regulate memory – independently of pathogens, cellular damage or disease(Ma et al.
78 2006, Rolls et al. 2007, Okun et al. 2010, Okun et al. 2011, Patel et al. 2016, Chen, CY et al. 2019). Whether

79 TLRs have functions in structural brain plasticity and behaviour remains little explored, and whether they
80 can function together with neurotrophins in the mammalian brain is unknown.

81 Progress linking cellular and molecular events to circuit and behavioural modification has been
82 rather daunting and limited using mammals(Wang et al. 2022). The *Drosophila* adult brain is plastic and can
83 be modified by experience and neuronal activity(Technau 1984, Barth and Heisenberg 1997, Barth et al.
84 1997, Sachse et al. 2007, Kremer et al. 2010, Sugie et al. 2015, Linneweber et al. 2020, Baltruschat et al.
85 2021, Coban et al. 2024). Different living conditions, stimulation with odorants or light, circadian rhythms,
86 nutrition, long-term memory and experimentally activating or silencing neurons, modify brain volume, alter
87 circuit and neuronal shape, and remodel synapses, revealing experience-dependent structural
88 plasticity(Devaud et al. 2001, Gorska-Andrzejak et al. 2005, Sachse et al. 2007, Fernandez et al. 2008,
89 Kremer et al. 2010, Bushey et al. 2011, Sugie et al. 2015, Duhart et al. 2020, Baltruschat et al. 2021,
90 Vaughen et al. 2022, Coban et al. 2024). Furthermore, the *Drosophila* brain is also susceptible to
91 neurodegeneration(Bolus et al. 2020). However, the molecular and circuit mechanisms underlying
92 structural brain plasticity are mostly unknown in *Drosophila*.

93 *Toll* receptors are expressed across the *Drosophila* brain, in distinct but overlapping patterns that
94 mark the anatomical brain domains(Li et al. 2020). Tolls share a common signalling pathway downstream,
95 that can drive at least four distinct cellular outcomes – cell death, survival, quiescence, proliferation –
96 depending on context(McIlroy et al. 2013, Foldi et al. 2017, Anthoney et al. 2018, Li et al. 2020). They are
97 also required for connectivity and structural synaptic plasticity and they can also induce cellular events
98 independently of signalling(McIlroy et al. 2013, Ward et al. 2015, McLaughlin et al. 2016, Foldi et al. 2017,
99 Ulian-Benitez et al. 2017, Li et al. 2020). These nervous system functions occur in the absence of tissue
100 damage or infection. This is consistent with the fact that - as well as universal functions in innate immunity
101 - Tolls also have multiple non-immune functions also outside the CNS, including the original discovery of
102 Toll in dorso-ventral patterning, cell intercalation, cell competition and others (Meyer et al. 2014, Pare et
103 al. 2014, Anthoney et al. 2018, Tamada et al. 2021). The Toll distribution patterns in the adult brain and

104 their ability to switch between distinct cellular outcomes means they are ideally placed to translate
105 experience into structural brain change(Li et al. 2020).
106 We had previously observed that in the adult brain, *Toll-6* is expressed in dopaminergic
107 neurons(McIlroy et al. 2013). Dopamine is a key neuromodulator that regulates wakefulness and
108 motivation, experience valence, such as reward, and it is essential for locomotion, learning and
109 memory(Riemensperger et al. 2011, Waddell 2013, Adel and Griffith 2021). In *Drosophila*, Dopaminergic
110 neurons (DANs) form an associative neural circuit together with mushroom body Kenyon cells (KCs), Dorsal
111 Anterior Lateral neurons (DAL) and Mushroom Body Output neurons (MBONs) (Chen, CC et al. 2012, Aso et
112 al. 2014a, Boto et al. 2020, Adel and Griffith 2021). Kenyon cells receive input from projection neurons of
113 the sensory systems, they then project through the mushroom body lobes where they are intersected by
114 DANs to regulate MBONs to drive behaviour (Heisenberg 2003, Aso et al. 2014b, Boto et al. 2020). This
115 associative circuit is required for learning, long-term memory and goal-oriented behaviour (Chen, CC et al.
116 2012, Guven-Ozkan and Davis 2014, Adel and Griffith 2021). During experience, involving sensory
117 stimulation from the external world and from own actions, dopamine assigns a value to otherwise neutral
118 stimuli, labelling the neural circuits engaged(Boto et al. 2020). Thus, this raises the possibility that a link of
119 Toll-6 to dopamine could enable translating experience into circuit modification to modulate behaviour.
120 In *Drosophila*, Toll receptors can function both independently of ligand-binding and by binding
121 Spätzle (Spz) protein family ligands, also known as *Drosophila* neurotrophins (DNTs), that are sequence,
122 structural and functional homologues of the mammalian NTs(DeLotto and DeLotto 1998, Weber et al. 2003,
123 Hoffmann et al. 2008a, Hoffmann et al. 2008b, Zhu et al. 2008, Lewis et al. 2013, McIlroy et al. 2013, Foldi
124 et al. 2017). Like mammalian NTs, DNTs also promote cell survival, connectivity, synaptogenesis and
125 structural synaptic plasticity, and they can also promote cell death, depending on context(Zhu et al. 2008,
126 McIlroy et al. 2013, Sutcliffe et al. 2013, Foldi et al. 2017, Ulian-Benitez et al. 2017). As well as Tolls, DNTs
127 are also ligands for Kekkon (Kek) receptors, kinase-less homologues of the mammalian NT Trk receptors
128 and are required for structural synaptic plasticity(Ulian-Benitez et al. 2017). Importantly, the targets
129 regulated by Tolls and Keks - ERK, NFκB, PI3K, JNK, CaMKII – are shared with those of mammalian NT

130 receptors Trk and p75^{NTR}, and have key roles in structural and functional plasticity across the animals (Park
131 and Poo 2013, Foldi et al. 2017, Ulian-Benitez et al. 2017, Yang et al. 2020, Tamada et al. 2021).
132 Here, we focus on Drosophila neurotrophin -2 (DNT-2), proved to be the ligand of Toll-6 and Kek-6,
133 with in vitro, cell culture and in vivo evidence (McIlroy et al. 2013, Foldi et al. 2017, Ulian-Benitez et al.
134 2017). Here we asked how DNT-2, Toll-6 and Kek-6 are functionally related to dopamine, whether they and
135 neuronal activity – as a proxy for experience - can modify neural circuits, and how structural circuit
136 plasticity modifies dopamine-dependent behaviours.
137
138 RESULTS
139 **DNT-2A, Toll-6 and Kek-6 neurons are integrated in a dopaminergic circuit**
140 To allow morphological and functional analyses of *DNT-2* expressing neurons, we generated a *DNT-2Gal4*
141 line using CRISPR/Cas9 and drove expression of the membrane-tethered-GFP *FlyBow1.1* reporter. We
142 identified at least 12 DNT-2+ neurons and we focused on four anterior DNT-2A neurons per hemi-brain
143 (Figure 1A). Using the post-synaptic marker Denmark, DNT-2A dendrites were found at the prow (PRW) and
144 flange (FLA) region, whereas axonal terminals visualised with the pre-synaptic marker synapse defective 1
145 (Dsyd1-GFP) resided at the superior medial protocerebrum (SMP) (Figure 1B,D). We additionally found
146 post-synaptic signal at the SMP and pre-synaptic signal at the FLA/PRW (Figure 1D), suggesting bidirectional
147 communication at both sites. Using Multi-Colour Flip-Out (MCFO) to label individual cells
148 stochastically(Nern et al. 2015, Costa et al. 2016), single neuron clones revealed variability in the DNT-2A
149 projections across individual flies (Figure 1C), consistently with developmental and activity-dependent
150 structural plasticity in *Drosophila*(Heisenberg et al. 1995, Kremer et al. 2010, Sugie et al. 2015, Mayseless et
151 al. 2018, Li et al. 2020, Linneweber et al. 2020, Baltruschat et al. 2021). We found that DNT-2A neurons are
152 glutamatergic as they express the vesicular glutamate transporter vGlut (Figure 1E, left) and lack markers
153 for other neurotransmitter types (Figure S1). DNT-2A terminals overlapped with those of dopaminergic
154 neurons (Figure 1F), suggesting they could receive inputs from neuromodulatory neurons. In fact, single-
155 cell RNA-seq revealed transcripts encoding the dopamine receptors *Dop1R1, Dop1R2, Dop2R* and/or

156 *DopEcR* in DNT-2+ neurons(Croset et al. 2018). Using reporters, we found that Dop2R is present in DNT-2A
157 neurons, but not Dop1R2 (Figure 1E right, Figure S1C). Altogether, these data showed that DNT-2A neurons
158 are excitatory glutamatergic neurons that could receive dopaminergic input both at PRW and SMP.
159 DNT-2 functions via Toll-6 and Kek-6 receptors, and *Toll-6* is expressed in DANs(McIlroy et al. 2013).
160 To identify the cells expressing *Toll-6* and *kek-6* and explore further their link to the dopaminergic system,
161 we used *Toll-6Gal4(Li et al. 2020)* and *kek-6Gal4*(Ulian-Benitez et al. 2017) to drive expression of
162 membrane-tethered *FlyBbow1.1* and assessed their expression throughout the brain. Using anti-Tyrosine
163 Hydroxilase (TH) - the enzyme that catalyses the penultimate step in dopamine synthesis - to visualise
164 DANs, we found that Toll-6+ neurons included dopaminergic neurons from the PAMs, PPL1 and PPL2
165 clusters (Figure 1H, Figure S2D,F Table S1), whilst Kek-6+ neurons included PAM, PAL, PPL1, PPM2 and
166 PPM3 dopaminergic clusters (Figure 1I, Figure S2B,E,F Table S1). DNT-2 can also bind various Tolls and Keks
167 promiscuously(McIlroy et al. 2013, Foldi et al. 2017) and other *Tolls* are also expressed in the dopaminergic
168 system: PAMs express multiple *Toll* receptors (Figure S2F) and all PPL1s express at least one *Toll* (Figure
169 S2F). Using MCFO clones revealed that both *Toll-6* and *kek-6* are also expressed in Kenyon cells (Li et al.
170 2020) (Figure S2I,J, Table S1), DAL neurons (Figure S2G,H, Table S1) and MBONs (Figure S2A-C). In summary,
171 *Toll-6* and *kek-6* are expressed in DANs, DAL, Kenyon cells and MBONs (Figure 1G). These cells belong to a
172 circuit required for associative learning, long-term memory and behavioural output, and DANs are also
173 required for locomotion (Riemensperger et al. 2011, Chen, CC et al. 2012, Aso et al. 2014b, Boto et al. 2014,
174 Adel and Griffith 2021). Altogether, our data showed that DNT-2A neurons are glutamatergic neurons that
175 could receive dopamine as they contacted DANs and expressed the *Dop2R* receptor, and that in turn DANs
176 expressed the DNT-2 receptors *Toll-6* and *kek-6*, and therefore could respond to DNT-2. These data
177 suggested that there could be bidirectional connectivity between DNT-2A neurons and DANs, which we
178 explored below.
179
180 **Bidirectional connectivity between DNT-2A neurons and DANs**

181 To verify the connectivity of DNT-2A neurons with DANs, we used various genetic tools. To identify DNT-2A
182 output neurons, we used TransTango(Talay et al. 2017) (Figure 2A and Figure S3). DNT-2A RFP+ outputs
183 included a subset of MB α'β' lobes, αβ Kenyon cells, tip of MB β'2, DAL neurons, dorsal fan-shaped body
184 layer and possibly PAM or other dopaminergic neurons (Figure 2A, see Figure S3). Consistently, these DNT-
185 2A output neurons express *Toll-6* and *kek-6* (Supplementary Table S1). To identify DNT-2A input neurons,
186 we used BAcTrace(Cachero et al. 2020). This identified PAM-DAN inputs at SMP (Figure 2B). Altogether,
187 these data showed that DNT-2A neurons receive dopaminergic neuromodulatory inputs, their outputs
188 include MB Kenyon cells, DAL neurons and possibly DANs, and DNT-2 arborisations at SMP are
189 bidirectional.

190 To further test the relationship between DNT-2A neurons and DANs, we reasoned that stimulating
191 DANs would provoke either release or production of dopamine. So, we asked whether increasing DNT-2
192 levels in DNT-2 neurons could influence dopamine levels. For this, we over-express *DNT-2* in full-length
193 form (i.e. *DNT-2FL*), as it enables to investigate non-autonomous functions of DNT-2 (Ulian-Benitez et al.
194 2017). Importantly, DNT-2FL is spontaneously cleaved into the mature form(McIlroy et al. 2013, Foldi et al.
195 2017) (see discussion). Thus, we over-expressed *DNT-2FL* in DNT-2 neurons and asked whether this
196 affected dopamine production, using mRNA levels for *TH* as readout. Using quantitative real-time PCR (qRT-
197 PCR) we found that over-expressing *DNT2-FL* in DNT-2 neurons in adult flies increased *TH* mRNA levels in fly
198 heads (Figure 2C). This showed that DNT-2 could stimulate dopamine production in neighbouring DANs.

199 Next, we wondered whether in turn DNT-2A neurons, that express *Dop2R*, could be modulated by
200 dopamine. Binding of dopamine to D2-like Dop2R (also known as DD2R) inhibits adenylyl-cyclase,
201 decreasing cAMP levels(Hearn et al. 2002, Neve et al. 2004). Thus, we asked whether DNT-2A neurons
202 received dopamine and signal via Dop2R. Genetic restrictions did not allow us to activate PAMs and test
203 DNT-2 neurons, so we activated DNT-2 neurons and tested whether *Dop2R* knock-down would increase
204 cAMP levels. We used the FRET-based cAMP sensor, Epac1-camps-50A(Shafer et al. 2008). When Epac1-
205 camps-50A binds cAMP, FRET is lost, resulting in decreased YFP/CFP ratio over time. Indeed, *Dop2R* RNAi
206 knock-down in DNT-2A neurons significantly increased cAMP levels (Figure 2D), demonstrating that

207 normally Dop2R inhibits cAMP signalling in DNT-2A cells. Importantly, this result meant that in controls,
208 activating DNT-2A neurons caused dopamine release from DANs that then bound Dop2R to inhibit adenylyl-
209 cyclase in DNT-2A neurons; this inhibition was prevented with *Dop2R* RNAi knock-down. Altogether, this
210 shows that DNT-2 up-regulated TH levels (Figure 2E), whereas dopamine inhibited cAMP in DNT-2A
211 neurons (Figure 2F).

212 In summary, DNT-2A neurons are connected to DANs, DAL and MB Kenyon cells, all of which
213 express DNT-2 receptors *Toll-6* and *kek-6* and belong to a dopaminergic as well as associative learning and
214 memory circuit. Furthermore, DNT-2A and PAM neurons form bidirectional connectivity. Finally, DNT-2 and
215 dopamine regulate each other: DNT-2 increased dopamine levels (Figure 2E), and in turn dopamine via
216 Dop2R inhibited cAMP signalling in DNT-2A neurons (Figure 2F). That is, an amplification was followed by
217 negative feedback. This suggested that a dysregulation in this feedback loop could have consequences for
218 dopamine-dependent behaviours and for circuit remodelling by the DNT-2 growth factor.

219

220 **DNT-2 and Toll-6 maintain survival of PAM dopaminergic neurons in the adult brain**

221 Above we showed that DNT-2 and PAM dopaminergic neurons are connected, so we next asked whether
222 loss of function for *DNT-2* or *Toll-6* would affect PAMs. In wild-type flies, PAM-DAN number can vary
223 between 220-250 cells per *Drosophila* brain, making them ideal to investigate changes in cell number(Liu et
224 al. 2012). Maintenance of neuronal survival is a manifestation of structural brain plasticity in mammals,
225 where it depends on the activity-dependent release of the neurotrophin BDNF(Lu et al. 2005, Wang et al.
226 2022). Importantly, cell number can also change in the adult fly, as neuronal activity can induce
227 neurogenesis via Toll-2, whereas DANs are lost in neurodegeneration models(Feany and Bender 2000, Li et
228 al. 2020). Thus, we asked whether DNT-2 influences PAM-DAN number in the adult brain. We used *THGal4;*
229 *R58E02Gal4* to visualise nuclear Histone-YFP in DANs (Figure 3A) and counted automatically YFP+ PAMs
230 using a purposely modified DeadEasy plug-in developed for the adult fly brain (Li et al 2020). DeadEasy
231 plug-ins were developed and used before to count cells labelled with sparsely distributed nuclear markers
232 in embryos(Zhu et al. 2008, Forero et al. 2009, Forero et al. 2010a, Forero et al. 2010b, McIlroy et al. 2013),

233 larvae(Kato et al. 2011, Forero et al. 2012, Losada-Perez et al. 2016) and adult(Li et al. 2020) *Drosophila*
234 brains. Here we show that *DNT2*^{37}/*DNT2*^{18} mutant adult brains had fewer PAMs than controls (Figure 3B).
235 Similarly, *Toll-6* RNAi knock-down in DANs also decreased PAM neuron number (Figure 3C). DAN loss was
236 confirmed with anti-TH antibodies and counted manually, as there were fewer TH+ PAMs in *DNT2*^{37}/*DNT2*^{18}
237 mutants (Figure 3D). Importantly, PAM cell loss was rescued by over-expressing activated *Toll-6*^{CY} in DANs
238 in *DNT-2* mutants (Figure 3D). Altogether, these data showed that DNT-2 functions via Toll-6 to maintain
239 PAM neuron survival.

240 To ask whether DNT-2 could regulate dopaminergic neuron number specifically in the adult brain,
241 we used *tubGal80*^{ts} to conditionally knock-down gene expression in the adult. PAMs were visualised with
242 either *R58E02LexA>LexAop-nls-tdTomato* or *THGal4; R58E02Gal4 >histone-YFP* and counted automatically.
243 Adult specific *DNT-2* RNAi knock-down decreased Tomato+ PAM cell number (Figure 3E). Similarly, RNAi
244 *Toll-6* knock-down in DANs also decreased PAM neuron number (Figure 3F). Furthermore, knock-down of
245 either *Toll-6* or *DNT-2* in the adult brain caused loss of PAM neurons visualised with anti-TH antibodies and
246 counted manually (Figure 3G). Cell loss was due to cell death, as adult specific *DNT-2 RNAi* knock-down
247 increased the number of apoptotic cells labelled with anti-*Drosophila* Cleave caspase-1 (DCP-1) antibodies
248 compared to controls (Figure 3H). This included Dcp-1+ PAMs (Figure 3H). By contrast, *DNT-2FL* over-
249 expression in DNT2 neurons did not alter the incidence of apoptosis (Figure 3G), consistently with the fact
250 that DNT-2FL spontaneously cleaves into the mature form(McIlroy et al. 2013, Foldi et al. 2017). Thus, *DNT-*
251 *2* and *Toll-6* knock-down specifically in the adult brain induced apoptosis and PAM-neuron loss.

252 Altogether, these data showed that sustained PAM neuron survival in development and in the adult
253 brain depends on DNT-2 and Toll-6, and a reduction in their levels causes DAN cell loss, characteristic of
254 neurodegeneration.

255

256 **DNT-2 and its receptors are required for arborisations and synapse formation**

257 We next asked whether DNT-2, Toll-6 and Kek-6 could influence dendritic and axonal arbours and synapses
258 of dopaminergic neurons (Figure 4A). Visualising the pre-synaptic reporter Synaptotagmin-GFP (Syt-GFP) in

259 PAM neurons, we found that *DNT-2^{18}/DNT-2^{37}* mutants completely lacked PAM synapses in the MB β,β' and
260 γ lobes (Figure 4B). Interestingly, PAM connections at α,α' lobes were not affected (Figure 4B). This means
261 that DNT-2 is required for synaptogenesis and connectivity of PAMs to MB β,β' and γ lobes.
262 PAM-β2β'2 neurons express *Toll-6* (Table S1) and their dendrites overlap axonal DNT2 projections.
263 *Toll-6* RNAi knock-down in PAM -β2β'2 (with split-GAL4 *MB301BGal4* (Aso et al. 2014a)), reduced dendrite
264 complexity (Figure 4C). To test whether DNT-2 could alter these dendrites, we over-expressed mature *DNT-*
265 *2CK*. DNT-2CK is not secreted (from transfected S2 cells), but it is functional in vivo(Zhu et al. 2008, Foldi et
266 al. 2017, Ulian-Benitez et al. 2017). Importantly, over-expressed *DNT-2CK* functions cell-autonomously
267 whereas *DNT-2FL* functions also non-autonomously, but they have similar effects(Zhu et al. 2008, Foldi et
268 al. 2017, Ulian-Benitez et al. 2017). Over-expression of *DNT-2CK* in PAM-β2β'2 increased dendrite arbour
269 complexity (Figure 4D). Thus, DNT-2 and its receptor Toll-6 are required for dendrite growth and complexity
270 in PAM neurons.
271 To ask whether DNT-2 could affect axonal terminals, we tested PPL1 axons. PPL1-γ1-pedc neurons
272 have a key function in long-term memory(Aso et al. 2012, Placais et al. 2012, Aso et al. 2014a, Boto et al.
273 2020) and express both *Toll-6* and *kek-6* (Table S1). Using split-GAL4 line M*B320C-Gal4* to visualise PPL1
274 axonal arbours, RNAi knock-down of either *Toll-6*, *kek-6* or both together caused axonal misrouting away
275 from the mushroom body peduncle (Figure 4E,E', Chi Square $p<0.05$, see Table S2). Similarly, *DNT-2FL* over-
276 expression also caused PPL1 misrouting (Figure 4F, Chi-Square $p<0.05$, see Table S2). Thus, DNT-2, Toll-6
277 and Kek-6 are required for appropriate targeting and connectivity of PPL1 DAN axons.
278 To test whether this signalling system was required specifically in the adult brain, we used *tubGAL80^{ts}*
279 to knock-down *Toll-6* and *kek-6* with RNAi conditionally in the adult and visualised the effect on
280 synaptogenesis using the post-synaptic reporter Homer-GCaMP and anti-GFP antibodies. Adult-specific
281 *Toll-6 kek-6* RNAi knock-down in PAM neurons did not affect synapse number (not shown), but it decreased
282 post-synaptic density size, both at the MB lobe and at the SMP dendrite (Figure 4G). These data meant that
283 the DNT-2 receptors *Toll-6* and *kek-6* continue to be required in the adult brain for appropriate
284 synaptogenesis.

285 Altogether, these data showed that DNT-2, Toll-6 and Kek-6 are required for dendrite branching,
286 axonal targeting and synapse formation. The shared phenotypes from altering the levels of *DNT-2* and *Toll-*
287 *6 kek-6* in arborisations and synapse formation, support their joint function in these contexts. Importantly,
288 these findings showed that connectivity of PAM and PPL1 dopaminergic neurons depend on DNT-2, Toll-6
289 and Kek-6.
290
291 **DNT-2 neuron activation and *DNT-2* over-expression induced synapse formation in target PAM**
292 **dopaminergic neurons**
293 The above data showed that DNT-2, Toll-6 and Kek-6 are required for DAN cell survival, arborisations and
294 synaptogenesis in development and adults. This meant that the dopaminergic circuit remains plastic in
295 adult flies. Thus, we wondered whether neuronal activity could also induce remodelling in PAM neurons.
296 In mammals, neuronal activity induces translation, release and cleavage of BDNF, and BDNF drives
297 synaptogenesis(Poo 2001, Lu et al. 2005, Lu et al. 2013, Wang et al. 2022). Thus, we first asked whether
298 neuronal activity could influence DNT-2 levels or function. We visualised tagged DNT-2FL-GFP in adult
299 brains, activated DNT-2 neurons with TrpA1 at 30°C, and found that DNT-2 neuron activation increased the
300 number of DNT-2-GFP vesicles produced (Supplementary Figure S4A). Furthermore, neuronal activity also
301 facilitated cleavage of DNT-2 into its mature form. In western blots from brains over-expressing *DNT-2FL-*
302 *GFP*, the levels of full-length DNT-2FL-GFP were reduced following neuronal activation and the cleaved
303 DNT-2CK-GFP form was most abundant (Supplementary Figure S4B). These findings meant that, like
304 mammalian BDNF, also DNT-2 can be influenced by activity.
305 Thus, we asked whether neuronal activity and DNT-2 could influence synapse formation. We first
306 tested DNT-2 neurons. Activating DNT-2 neurons altered DNT-2 axonal arbours (Figure 5A) and it increased
307 Homer-GFP+ synapse number in the DNT-2 SMP arbour (Figure 5B and Figure S5). Next, as DNT-2 and PAMs
308 form bidirectional connexions at SMP (Figure 1, 2), we asked whether activating DNT-2 neurons could
309 affect target PAM neurons. To manipulate DNT-2 neurons and visualise PAM neurons concomitantly, we
310 combined *DNT-2GAL4* with the *PAM-LexAOP* driver. However, there were no available *LexA/OP* post-

311 synaptic reporters, so we used the pre-synaptic *LexAOP-Syt-GCaM*P reporter instead, which labels
312 Synaptotagmin (Syt), and GFP antibodies. Activating DNT-2 neurons with TrpA1 increased the number of
313 Syt+ synapses at the PAM SMP arbour (Figure 5C) and reduced their size (Figure 5C). This was consistent
314 with the increase in Homer-GFP+ PSD number in stimulated DNT-2 neurons (Figure 5B). Neuronal activity
315 can induce ghost boutons, immature synapses that are later eliminated (Fuentes-Medel et al. 2009). Here,
316 the coincidence of increased pre-synaptic Syt-GFP from PAMs and post-synaptic Homer-GFP from DNT-2
317 neurons at SMP revealed that newly formed synapses were stable. PAM neurons also send an arborisation
318 at the MB β, β', γ lobes, but DNT-2 neuron activation did not affect synapse number nor size there (Figure
319 5C). These data showed that activating DNT-2 neurons induced synapse formation at the SMP connection
320 with PAMs.

321 Finally, we asked whether, like activity, DNT-2FL could also drive synaptogenesis. We over-expressed
322 *DNT-2FL* in DNT-2 neurons and visualised the effect in PAM neurons. Over-expression of *DNT-2FL* in DNT-2
323 neurons did not alter Syt+ synapse number at the PAM SMP dendrite, but it increased bouton size (Figure
324 5D). By contrast, at the MB β, β' lobe arborisation, over-expressed *DNT-2* did not affect Syt+ bouton size,
325 but it increased the number of output synapses (Figure 5D). This data showed that DNT-2 released from
326 DNT-2 neurons could induce synapse formation in PAM target neurons.

327 Altogether, these data showed that neuronal activity induced synapse formation, it stimulated
328 production and cleavage of DNT-2, and DNT-2 could induce synapse formation in target neurons.

329

330 **Structural plasticity by DNT2 modified dopamine-dependent behaviour**

331 Circuit structural plasticity raises the important question of what effect it could have on brain function, i.e.
332 behaviour. Data above showed that DANs and DNT-2 neurons are functionally connected, that loss of
333 function for *DNT-2* or its receptors caused dopaminergic neuron loss, altered DAN arborisations and caused
334 synapse loss or reduction in size, and that DNT-2 could induce dendrite branching and synaptogenesis,
335 altogether modifying circuit connectivity. To measure the effect of such circuit modifications on brain
336 function, we used dopamine-dependent behaviours as readout.

337 Startle-induced negative geotaxis (also known as the climbing assay) is commonly used as a
338 measure of locomotor ability and requires dopamine and specifically PAM neuron function(Riemensperger
339 et al. 2013, Sun et al. 2018). We tested the effect of *DNT-2* or *Toll-6* and *kek-6* loss of function in climbing,
340 and both *DNT-2*^{37}/*DNT-2*^{18} mutants and flies in which *DNT-2* was knocked-down in DNT-2 neurons in the
341 adult stage had lower climbing ability than controls (Figure 6A). Similarly, when *Toll-6* and *kek-6* were
342 knocked-down with RNAi in the adult using a *Toll-6-* or a *PAM-GAL4* neuron driver, climbing was also
343 reduced (Figure 6B). Importantly, over-expressing activated *Toll-6*^{CY} in DANs rescued the locomotion
344 deficits of *DNT-2* mutants, showing that DNT-2 functions via Toll-6 in this context (Figure 6C).
345 We also tracked freely moving flies in an open arena(Eyjolfsdottir et al. 2014). Interestingly, in that
346 setting, locomotion of homozygous *DNT-2*^{37}/*DNT-2*^{18} mutants was similar to that of controls, but over-
347 expression of *Toll-6*^{CY} in their DANs increased locomotion as flies walked longer distances and spent less
348 time immobile (Figure 6D). Adult flies over-expressing *DNT2-FL* walked faster (Figure 6E and Figure S5) and
349 so did those where DNT-2 neurons were activated with TrpA1 (Figure 6F and Figure S6), consistently with
350 the fact that neuronal activity increased DNT-2 production (Figure S4A) and that DNT-2FL increased TH
351 levels (Figure 2C). Therefore, increased Toll-6^{CY} levels in DANs increase locomotion and increased DNT-2
352 levels are sufficient to boost walking speed. Interestingly, both loss and gain of function for *DNT-2* also
353 caused seizures (Figure S7). Thus, dopamine-dependent locomotion is regulated by the function of DNT-2,
354 Toll-6 and Kek-6.
355 Next, as dopamine is an essential neurotransmitter for learning and memory(Adel and Griffith
356 2021), we asked whether DNT-2 might influence appetitive olfactory conditioning. Starved flies were
357 trained to associate a sugar reward with an odour (CS+) while another odour was presented without sugar
358 (CS-), and their preference for CS+ versus CS- was measured, 24h after training (as in (Krashes and Waddell
359 2008, 2011)). Remarkably, over-expression of *DNT-2FL* in DNT-2 neurons in adults enhanced appetitive
360 long-term memory (Figure 6G), consistent with the positive role of DNT-2 in synaptogenesis that we
361 demonstrated above.

362 In summary, we have shown that alterations in DNT-2, Toll-6 and Kek-6 levels that caused
363 structural phenotypes in DANs also modified dopamine-dependent behaviours, locomotion and long-term
364 memory.
365
366 DISCUSSION
367 Our findings indicate that structural plasticity and degeneration in the brain are two manifestations of a
368 shared molecular mechanism that could be modulated by experience. Loss of function for *DNT-2, Toll-6* and
369 *kek-6* caused cell loss, affected arborisations and synaptogenesis in DANs and impaired locomotion;
370 neuronal activity increased DNT-2 production and cleavage and remodelled connecting DNT-2 and PAM
371 synapses; and over-expression of *DNT-2* increased TH levels, PAM dendrite complexity, and synaptogenesis,
372 and it enhanced locomotion and long-term memory.
373 It was remarkable to find that dopaminergic neurons in the *Drosophila* adult brain require
374 sustained trophic support, and this is functionally relevant as it can influence behaviour. Loss of *DNT-2*
375 function in mutants, constant loss of *Toll-6* function in DANS and adult-restricted knock-down of either
376 *DNT-2* (in DNT-2 neurons) or *Toll-6* (in Toll-6 neurons and in DANs) all resulted in DAN cell loss, verified with
377 three distinct reporters, and consistently with the increase in DAN apoptosis. Furthermore, DAN cell loss in
378 *DNT-2* mutants could be rescued by the over-expression of *Toll-6* in DANs. Cell loss was also verified using
379 two reporter types (ie GAL4 based nuclear reporters and cytoplasmic anti-TH antibodies), multiple GAL4
380 drivers and mutants, and multiple cell counting methods, including automatic cell counting with DeadEasy
381 plug-ins for His-YFP and nls-Tomato (where the signal was of high contrast and sphericity) and software
382 assisted manual cell counting for anti-TH (where the signal is more diffuse and less regular in shape).
383 DeadEasy plug-ins have been used before for reliably counting His-YFP labelled cells in both larval CNS and
384 adult brains, including Kenyon cells (Kato et al. 2011, Forero et al. 2012, Losada-Perez et al. 2016, Li et al.
385 2020, Harrison et al. 2021). Thus, the finding that loss of *DNT-2* and *Toll-6* function in the adult brain cause
386 dopaminergic neuron loss is robust. Our findings are reminiscent of the increased apoptosis and cell loss in
387 adult brains with *Toll-2* loss of function(Li et al. 2020), and the support of DAN survival by Toll-1 and Toll-7

388 driven autophagy(Zhang et al. 2024). They are also consistent with a report that loss of function for *DNT-2*
389 or *Toll-6* induced apoptosis in the third instar larval optic lobes(McLaughlin et al. 2019). This did not result
390 in neuronal loss - which was interpreted as due to Toll-6 functions exclusive to glia (McLaughlin et al. 2019)
391 - but instead of testing the optic lobes, neurons of the larval abdominal ventral nerve cord (VNC) were
392 monitored(McLaughlin et al. 2019). In the VNC, Toll-6 and -7 function redundantly and knock-down of both
393 is required to cause neuronal loss in embryos(McIlroy et al. 2013), whereas in L3 larvae and pupae the
394 phenotype is compounded by their pro-apoptotic functions(Foldi et al. 2017). It is crucial to consider that
395 the DNT-Toll signalling system can have distinct cellular outcomes depending on context, cell type and
396 time, ie stage (Foldi et al. 2017, Li et al. 2020, Li and Hidalgo 2021). Our work shows that in the adult
397 *Drosophila* brain DAN neurons receive secreted growth factors that maintain cellular integrity, and this
398 impacts behaviour. Consistently with our findings, *Drosophila* models of Parkinson's Disease reproduce the
399 loss of DANs and locomotion impairment of human patients(Feany and Bender 2000, Riemensperger et al.
400 2011, Riemensperger et al. 2013, Sun et al. 2018). Dopamine is required for locomotion, associative reward
401 learning and long-term memory(Riemensperger et al. 2011, Riemensperger et al. 2013, Waddell 2013, Sun
402 et al. 2018, Boto et al. 2020, Adel and Griffith 2021). In *Drosophila*, this requires PAM, PPL1 and DAL
403 neurons and their connections to Kenyon Cells and MBONs(Heisenberg 2003, Chen et al. 2012, Aso et al.
404 2014b, Boto et al. 2020, Adel and Griffith 2021). DNT-2 neurons are connected to all these neuron types,
405 which express *Toll-6* and *kek-6,* and modifying their levels affected locomotion and long-term memory.
406 Altogether, our data demonstrate that structural changes caused by altering DNT-2, Toll-6 and Kek-6
407 modified dopamine-dependent behaviours, providing a direct link between molecules, structural circuit
408 plasticity and behaviour.

409 We used neuronal activation as a proxy for experience, but the implication is that experience would
410 similarly drive the structural modification of circuits labelled by neuromodulators. Similar manipulations of
411 activity have previously revealed structural circuit modifications. For example, hyperpolarising olfactory
412 projection neurons increased microglomeruli number, active zone density and post-synaptic site size in the
413 calyx, whereas inhibition of synaptic vesicle release decreased the number of microglomeruli and active

414 zones(Kremer et al. 2010). There is also evidence that experience can modify circuits and behaviour in
415 *Drosophila.* For example, natural exposure to light and dark cycles maintains the structural homeostasis of
416 presynaptic sites in photoreceptor neurons, which breaks down in sustained exposure to light(Sugie et al.
417 2015). Prolonged odour exposure causes structural reduction at the antennal lobe and at the output pre-
418 synaptic sites in the calyx, and habituation (Devaud et al. 2001, Pech et al. 2015). Similarly, prolonged
419 exposure to CO2 caused a reduction in output responses at the lateral horn and habituation(Sachse et al.
420 2007). Our findings are also consistent with previous reports of structural plasticity during learning in
421 *Drosophila.* Hypocaloric food promotes structural plasticity in DANs, causing a reduction specifically in
422 connections between DANs and Kenyon cells involved in aversive learning, thus decreasing the memory of
423 the aversive experience(Coban et al. 2024). By contrast, after olfactory conditioning, appetitive long-term
424 memory increased axonal collaterals in projection neurons, and synapse number at Kenyon cell inputs in
425 the calyx(Baltruschat et al. 2021). Our data provide a direct link between a molecular mechanism, synapse
426 formation in a dopaminergic circuit and behavioural performance. Since behaviour is a source of
427 experience, the discovery that a neurotrophin can function with a Toll and a neuromodulator to sculpt
428 circuits provides a mechanistic basis for how experience can shape the brain throughout life.
429 Importantly, in humans structural brain plasticity (e.g. adult neurogenesis, neuronal survival,
430 neurite growth and synaptogenesis) correlates with anti-depressant treatment, learning, physical exercise
431 and well-being(Cotman and Berchtold 2002, Woollett and Maguire 2011, Castren and Monteggia 2021,
432 Cheng et al. 2022). Conversely, neurite, synapse and cell loss, correlate with ageing, neuroinflammation,
433 psychiatric and neurodegenerative conditions(Holtmaat and Svoboda 2009, Lu et al. 2013, Wohleb et al.
434 2016, Forrest et al. 2018, Vahid-Ansari and Albert 2021, Wang et al. 2022). Understanding how experience
435 drives the switch between generative and destructive cellular processes shaping the brain is critical to
436 understand brain function, in health and disease. In this context, the mechanism we have discovered could
437 also operate in the human brain. In fact, there is deep evolutionary conservation in DNT-2 vs mammalian
438 NT function (eg BDNF), but some details differ. Like mammalian NTs, full-length DNTs/Spz proteins contain
439 a signal peptide, an unstructured pro-domain and an evolutionarily conserved cystine-knot of the NT

440 family(Zhu et al. 2008, Arnot et al. 2010, Foldi et al. 2017). Cleavage of the pro-domain releases the mature
441 cystine-knot (CK). In mammals, full-length NTs have opposite functions to their cleaved forms (e.g.
442 apoptosis vs cell survival, respectively). However, DNT-2FL is cleaved by intracellular furins, and although
443 DNT-2 can be found both in full-length or cleaved forms in vivo, it is most abundantly found cleaved(Zhu et
444 al. 2008, McIlroy et al. 2013, Foldi et al. 2017). As a result, over-expressed *DNT-2FL* does not induce
445 apoptosis and instead it promotes cell survival(Foldi et al. 2017). The same functions are played by over-
446 expressed mature *DNT-2CK* as by *DNT-2FL*(Zhu et al. 2008, Foldi et al. 2017, Ulian-Benitez et al. 2017). In S2
447 cells, transfected DNT-2CK is not secreted, but when over-expressed in vivo it is functional (Zhu et al. 2008,
448 Foldi et al. 2017, Ulian-Benitez et al. 2017) (and this work). In fact, over-expressed *DNT-2CK* also maintains
449 neuronal survival, connectivity and synaptogenesis(Zhu et al. 2008, Foldi et al. 2017, Ulian-Benitez et al.
450 2017) (and this work). Similarly, over-expressed mature *spz-1-C106* can rescue the *spz-1*-null mutant
451 phenotype(Hu et al. 2004) and over-expressed *DNT-1CK* can promote neuronal survival, connectivity and
452 rescue the *DNT-1* mutant phenotype(Zhu et al. 2008). Consistently, both DNT-2FL and DNT-2CK have neuro-
453 protective functions promoting cell survival, neurite growth and synaptogenesis(Zhu et al. 2008, Sutcliffe et
454 al. 2013, Foldi et al. 2017, Ulian-Benitez et al. 2017) (and this work). Importantly, over-expressing *DNT-2FL*
455 enables to investigate non-autonomous functions of DNT-2(Ulian-Benitez et al. 2017). We have shown that
456 *DNT-2FL* can induce synaptogenesis non-autonomously in target neurons. Similarly, DNT-2 is a retrograde
457 factor at the larval NMJ, where transcripts are located post-synaptically in the muscle, DNT-2FL-GFP is
458 taken up from muscle by motorneurons, where it induces synaptogenesis(Sutcliffe et al. 2013, Ulian-
459 Benitez et al. 2017). Importantly, we have shown that neuronal activity increased production of tagged
460 DNT-2-GFP, and its cleavage. In mammals, neuronal activity induces synthesis, release and cleavage of
461 BDNF, leading to neuronal survival, dendrite growth and branching, synaptogenesis and synaptic plasticity
462 (ie LTP)(Poo 2001, Horch and Katz 2002, Lu et al. 2005, Arikkath 2012, Wang et al. 2022). Like BDNF, DNT-2
463 also induced synaptogenesis and increased bouton size. It may not always be possible to disentangle
464 primary from compensatory phenotypes, as Hebbian, homeostatic and heterosynaptic plasticity can
465 concur(Forrest et al. 2018, Jenks et al. 2021). Mammalian BDNF increases synapse number, spine size and

466 long-term potentiation (LTP), but it can also regulate homeostatic plasticity and long-term depression
467 (LTD), depending on timing, levels and site of action(Poo 2001, Lu et al. 2005, Wang et al. 2022). In this
468 context, neuronal stimulation of DNT-2 neurons induced synapse formation in PAM neuron SMP dendrites,
469 whereas DNT-2 over-expression from DNT-2 neurons increased synapse size at SMP and synapse number in
470 PAM outputs at the mushroom body lobes. These distinct effects could be due to the combination of
471 plasticity mechanisms and range of action. Neuronal activity can induce localised protein synthesis that
472 facilitates local synaptogenesis and stabilises emerging synapses(Forrest et al. 2018). By contrast, DNT-2
473 induced signalling via the nucleus can facilitate synaptogenesis at longer distances, in output sites. In any
474 case, synaptic remodelling is the result of concurring forms of activity-dependent plasticity altogether
475 leading to modification in connectivity patterns(Forrest et al. 2018, Jenks et al. 2021). Long-term memory
476 requires synaptogenesis, and in mammals this depends on BDNF, and its role in the protein-synthesis
477 dependent phase of LTP(Poo 2001, Minichiello 2009, Wang et al. 2022). BDNF localised translation,
478 expression and release are induced to enable long-term memory(Poo 2001, Lee et al. 2004, Minichiello
479 2009, Wang et al. 2022). We have shown that similarly, over-expressed *DNT-2FL* increased both
480 synaptogenesis in sites involved in reward learning, and long-term memory after appetitive conditioning.
481 The relationship of NTs with dopamine is also conserved. DNT-2 and DAN neurons form
482 bidirectional connectivity that modulates both DNT-2 and dopamine levels. Similarly, mammalian NTs also
483 promote dopamine release and the expression of DA receptors(Blochl and Sirrenberg 1996, Guillin et al.
484 2001). Furthermore, DAN cell survival is maintained by DNT-2 in *Drosophila,* and similarly DAN cell survival
485 is also maintained by NT signalling in mammals and fish(Hyman et al. 1991, Sahu et al. 2019). Importantly,
486 we showed that activating DNT-2 neurons increased the levels and cleavage of DNT-2, up-regulated DNT-2
487 increased *TH* expression, and this initial amplification resulted in the inhibition of cAMP signalling by
488 dopamine via Dop2R in DNT-2 neurons. This negative feedback could drive a homeostatic reset of both
489 DNT-2 and dopamine levels, important for normal brain function. In fact, alterations in DNT-2 levels could
490 cause seizures. Importantly, alterations in both NTs and dopamine underlie many psychiatric disorders and

491 neurodegenerative diseases in humans(Hyman et al. 1991, Guillin et al. 2001, Berton et al. 2006, Forrest et
492 al. 2018, Wang et al. 2022).

493 We have uncovered a novel mechanism of structural brain plasticity, involving a NT ligand
494 functioning via a Toll and a kinase-less Trk-family receptor in the adult *Drosophila* brain. Toll receptors in
495 the CNS can function via ligand dependent and ligand-independent mechanisms(Anthoney et al. 2018).
496 However, in the context analysed, Toll-6 and Kek-6 function in structural circuit plasticity depends on their
497 ligand DNT-2. This is also consistent with their functions promoting axonal arbour growth, branching and
498 synaptogenesis at the NMJ(Ulian-Benitez et al. 2017). Furthermore, Toll-2 is also neuro-protective in the
499 adult fly brain, and loss of *Toll-2* function caused neurodegeneration and impaired behaviour (Li et al.
500 2020). There are six *spz/DNT*, nine *Toll* and six *kek* paralogous genes in *Drosophila*(Tauszig et al. 2000,
501 MacLaren et al. 2004, Mandai et al. 2009, Ulian-Benitez et al. 2017), and at least seven *Tolls* and three
502 adaptors are expressed in distinct but overlapping patterns in the brain (Li et al. 2020). Such combinatorial
503 complexity opens the possibility for a fine-tuned regulation of structural circuit plasticity and homeostasis
504 in the brain.

505 *Drosophila* and mammalian NTs may have evolved to use different receptor types to elicit
506 equivalent cellular outcomes. In fact, in mammals, NTs function via Trk, $p75^{NTR}$ and Sortilin receptors, to
507 activate ERK, PI3K, NFκB, JNK and CaMKII(Lu et al. 2005, Wang et al. 2022). Similarly, DNTs with Tolls and
508 Keks also activate ERK, NFκB, JNK and CaMKII in the *Drosophila* CNS(McIlroy et al. 2013, Foldi et al. 2017,
509 Ulian-Benitez et al. 2017, Anthoney et al. 2018). However, alternatively, NTs may also use further receptors
510 in mammals. Trks have many kinase-less isoforms, and understanding of their function is limited(Fryer et al.
511 1996, Stoilov et al. 2002). They can function as ligand sinks and dominant negative forms, but they can also
512 function independently of full-length Trks to influence calcium levels, growth cone extension and dendritic
513 growth and are linked to psychiatric disorders, e.g. depression(Ferrer et al. 1999, Yacoubian and Lo 2000,
514 Ohira et al. 2006, Carim-Todd et al. 2009, Ernst et al. 2009, Ohira and Hayashi 2009, Fenner 2012,
515 Tessarollo and Yanpallewar 2022). Like Keks, perhaps kinase-less Trks could regulate brain plasticity vs.
516 degeneration. A functional relationship between NTs and TLRs could exist also in humans, as in cell culture,

517 human BDNF and NGF can induce signalling from a TLR(Foldi et al. 2017) and NGF also functions in
518 immunity and neuroinflammation(Levi-Montalcini et al. 1996, Hepburn et al. 2014). Importantly, TLRs can
519 regulate cell survival, death and proliferation, neurogenesis, neurite growth and collapse, learning and
520 memory(Okun et al. 2011). They are linked to neuroinflammation, psychiatric disorders, neurodegenerative
521 diseases and stroke(Okun et al. 2011, Figueroa-Hall et al. 2020, Adhikarla et al. 2021). Intriguingly, genome-
522 wide association studies (GWAS) have revealed the involvement of TLRs in various brain conditions and
523 potential links between NTs and TLRs in, for example, major depression(Sharma 2012, Mehta et al. 2018,
524 Chan et al. 2020, Garrett et al. 2021). Importantly, alterations in NT function underlie psychiatric,
525 neurologic and neurodegenerative brain diseases(Lu et al. 2005, Martinowich et al. 2007, Krishnan and
526 Nestler 2008, Lu et al. 2013, Park and Poo 2013, Wohleb et al. 2016, Yang et al. 2020, Casarotto et al. 2021,
527 Wang et al. 2022) and BDNF underlies the plasticity inducing function of anti-depressants(Lu et al. 2013,
528 Casarotto et al. 2021, Wang et al. 2022). It is compelling to find out whether and how these important
529 protein families – NTs, TLRs and kinase-less Trks - interact in the human brain.
530
531 **Conclusion**
532 To conclude, we provide a direct link between structural circuit plasticity and behavioural performance, by
533 a novel molecular mechanism. The neurotrophin DNT-2 and its receptors Toll-6 and the kinase-less Trk
534 family Kek-6 are linked to a dopaminergic circuit. Neuronal activity boosts DNT-2, and DNT-2 and dopamine
535 regulate each other homeostatically. Dopamine labels the circuits engaged and DNT-2, a growth factor,
536 with its receptors Toll-6 and Kek-6, drives structural plasticity in these circuits, enhancing dopamine-
537 dependent behavioural performance. These findings mean that DNT-2 is a plasticity factor in the *Drosophila*
538 brain enabling experience-dependent behavioural enhancement. Whether NTs can similarly functions with
539 TLRs and Kinase-less Trks remains to be explored. As behaviour is a source of experience, this has profound
540 implications for understanding brain function and health.
541
542 ACKNOWLEDGEMENTS

We thank our lab, Carolina Rezaval and Thomas Riemensperger for comments on the manuscript; Carolina Rezaval, Reinhard Wolf, Martin Heisenberg and Scott Waddell for advice on - Karina Piotrowska for help with - behaviour experiments; Xiufeng Li for help with programming; Serge Birman, Ann-Shyn Chiang, Ron Davis, André Fialá, Barret Pfeiffer, Xi Rao, Carolina Rezaval, Iris Salecker for flies; DSHB (Iowa) for antibodies; AddGene for plasmids; Bloomington Stock Centre for *Drosophila* stocks. This work was funded by Marie-Curie Sklodowska Post-Doctoral fellowship to J.S.; Science Without Borders-CAPES PhD Studentship BEX 13380/13-3 to SUB; BBSRC Project Grants BB/R00871X/1 and BB/P004997/1 to A.H.; and Wellcome Trust Investigator Award 223197/Z/21/Z to A.H.

AUTHOR CONTRIBUTIONS

J.S., V.C designed and A.H. executed experiments and/or analysed data; S.U-B, G.L, D.S, X.W., F.R.C, M.M. executed experiments and analysed data; M.G.F, S.C., A.H. developed tools; D.K., G.J, V.C., A.H. supervised; J.S and A.H. wrote the manuscript. A.H. conceived and directed the project. All authors provided feedback on, and contributed to improvements to, the manuscript.

DATA AVAILABILITY STATEMENT

All data are contained within the manuscript; metadata and statistical analysis details including full genotypes, sample sizes, statistical tests and p values have been provided in Table S2. This work generated fly stocks and molecular constructs, which we will distribute on request. Raw data will be distributed on request.

DECLARATION OF INTERESTS

The authors declare that they have no conflict of interest.

MATERIALS AND METHODS

Genetics

570 **Mutants:** *DNT2*^{37} and *DNT2*^{18} are protein null(Foldi et al. 2017, Ulian-Benitez et al. 2017). *Toll6*^{31} is a null
571 mutant allele(McIlroy et al. 2013). **Driver lines:** *DNT2-Gal4* is a CRISPR/Cas9-knock-in allele, with GAL4 at
572 the start of the gene (this work, see below). *Toll-6-Gal4* was generated by RMCE from *MIMIC Toll-6*^{MIO2127}*;*
573 *kek6-Gal4* from *MIMIC Kek6*^{MI12953}(Ulian-Benitez et al. 2017, Li et al. 2020). *MB320C-Gal4 (BSC68253),*
574 *MB301B-Gal4 (BSC68311), R58E02-Gal4 (BSC41347), MB247-Gal80 (BSC64306), R58E02-LexA (BSC52740),*
575 *R14C08-LexA (BSC52473)* were from the *Drosophila* Bloomington Stock Centre (BSC). *Dop1R2-LexA, Dop2R-*
576 *LexA, Gad-LexA* were kindly provided by Yi Rao; *TH-LexA* (gift of Ron Davis), *TH-Gal4,R58E02-GAL4* (gift of
577 Serge Birman); *G0431-Gal4 (DAL-GAL4), VT49239 nls LexA (DAL LexA)* (gifts from Ann-Shyn Chiang);
578 tubGal80ts, Tdc-LexA. **Reporter lines:** *UAS-CD8::GFP,* for membrane tethered GFP; *UAS-histone-YFP*, for
579 YFP-tagged nuclear histone; *UASFlybow1.1*, constant membrane tethered expression (gift of Iris Salecker);
580 *13xLexAop-nls-tdTomato,* nuclear Tomato (gift of B. Pfeiffer); *UASCD8::RFP, LexAopCD8::GFP* (BSC32229),
581 for dual binary expression; *UAS-homer-GCaMP* for post-synaptic densities (gift of André Fialá), *UAS-*
582 *syt.eGFP* (BSC6925) and *LexAop-Syt-GCaMP* (BSC64413) for presynaptic sites. **For connectivity***: UAS-*
583 *DenMarkRFP, UAS-Dsyd1GFP* (gift of Carolina Rezaval); TransTango: *yw UAS-myrGFP,QUAS-mtdTomato-*
584 *3xHA attP8; Trans-Tango@attP40* (BSC77124); BAcTrace 806 *(w;LexAop2-Syb::GFP-P10(VK37) LexAop-*
585 *QF2::SNAP25::HIVNES::Syntaxin(VK18)/CyO; UAS-B3Recombinase (attP2) UAS<B3Stop<BoNT/A (VK5)*
586 *UAS<B3Stop<BoNT/A(VK27) QUAS-mtdTomato::HA/TM2*): **MCFO clones**: *hs-FLPG5.PEST;; 10xUAS*
587 *(FRT.stop) myr::smGdP-OLLAS 10xUAS (FRT.stop) myr::smGdP-HA 10xUAS (FRT.stop) myr::smGdP-V5-THS-*
588 *10xUAS (FRT.stop) myr::smGdP-FLAG* (BSC64086). **Optogenetic activation:** *20x UAS-V5-Syn-CsChrimson td*
589 *tomato* (gift of B. Pfeiffer**). For thermogenetic activation:** *UASTrpA1@attP2 (BSC26264)* and *UAS-*
590 *TrpA1@attP216 (BSC26263).* **UAS gene over-expression**: *UAS-DNT2CK, UAS-DNT2FL-GFP, UAS-DNT2-FL-*
591 *47C, UAS-Toll-6*^{CY}(McIlroy et al. 2013, Foldi et al. 2017). **UAS-RNAi knockdown:** *UAS-DNT2RNAi*
592 (VDRC49195), *UAS-Toll6RNAi* (VDRC928), *y*^{1}*v*^{1}*; UAS-Toll6RNAi[Trip.HMS04251]* (BSC 56048*), UAS-kek6RNAi*
593 (VDCR 109681), *y*^{1}*v*^{1}*; UAS-Dop2R-RNAi[TRiP.HMC02988](*BSC50621).
594
595 **Molecular biology**

596 *DNT-2GAL4* was generated by CRISPR/Cas9 enhanced homologous recombination. 1 kb long 5' and 3'
597 homology arms (HA) were amplified by PCR from genomic DNA of wild type flies, using primers for 5'HA:
598 atcgcaccggtttttacaggcaccccatgtctga containing AgeI cutting site and
599 cttgacgcggccgcTGTCAATTCATTCGCCGTCGAT containing NotI cutting site. 3'HA primers were:
600 tattaggcgcgccATGACAAAAAGTATTAAACGTCCGCCC containing AscI cutting site and
601 tactcgactagtgaagcacacccaaaatacccagg containing SpeI cutting site. HAs were sequentially cloned by
602 conventional cloning into pGEM-T2AGal4 vector (Addgene #62894). For gRNA cloning, two 20 nucleotide
603 gRNA oligos (gtcGACAAGTTCTTCTTACCTATG and aaacCATAGGTAAGAAGAACTTGTC) were designed using
604 Optimal Target Finder. BbsI enzyme sites were added: gtc(g) at the 5' end of sense oligo, and aaac at the 5'
605 end of the antisense oligo. gRNA is located at 41 bp downstream of the start codon of DNT-2 within the
606 first coding exon. The gRNA was cloned into pU6.3 using conventional ligation. The two constructs were
607 injected in Cas9 bearing flies and red fluorescent (3xP3-RFP) transformants were selected and balanced,
608 after which 3xP3-RFP was removed with CRE-recombinase.
609
610 **qRT-PCR**
611 qRT-PCR was carried out from 20 whole adult fruit-fly heads, frozen in liquid nitrogen before homogenising
612 in 50 ml Trizol (Ambion #AM9738), followed by a stand RNA extraction protocol. RNA was treated with
613 DNase treatment (ThermoFisher # AM1906) to remove genomic DNA. 200 ng of RNA was used for cDNA
614 synthesis following Goscript Reverse Transcriptase (Promega #237815) protocol. Sample was diluted 1:4
615 with Nuclease free H_2O. Standard qPCR was performed with SensiFast syb Green Mix (Bioline #B2092020)
616 in ABI qPCR plate (GeneFlow #P3-0292) and machine. To amplify TH mRNA the following primers were
617 used: TH-F: CGAGGACGAGATTTTGTTGGC and TH-R: TTGAGGCGGACCACCAAAG. GAPDH was used as a
618 housekeeping control. Reactions were performed in triplicate. Specificity and size of amplification products
619 were assessed by melting curve analyses. Target gene expression relative to reference gene is expressed as
620 value of $2^{-\Delta\Delta Ct}$ (where Ct is the crossing threshold).
621

622 **Conditional expression**

623 **Multiple Colour Flip Out clones:** *DNT2-Gal4, Toll6-Gal4* and *kek6-Gal4* were crossed with
624 *hsFLP::PEST;;MCFO* flies, female offspring were collected and heat-shocked at 37°C in a water bath for 15
625 mins, then kept for 48h at 25°C before dissecting their brains. ***TransTango:*** DNT2-Gal4 or Oregon female
626 virgins were crossed with *TransTango* males, progeny flies were raised at 18°C constantly and 15 days after
627 eclosion, female flies were selected for immunostaining. **Thermogenetic activation with *TrpA1:*** Fruit-flies
628 were bred at 18°C from egg laying to 4 days post-adult eclosion, then shifted to 29°C in a water bath for
629 24h followed by 24h recovery at room temperature for over-expressed *DNT-2FL-GFP*; for the other
630 experiments, after breeding as above, adult flies were transferred to an incubator at 30°C, kept there for
631 24h and then brains were dissected. **Conditional gene over-expression and RNAi knockdown:** Flies bearing
632 the temperature sensitive GAL4 repressor tubGal80^{ts} were kept at 18°C from egg laying to adult eclosion,
633 then transferred to 30 °C incubator for 48h for Dcp-1+ and cell counting experiments and for 120h for TH+
634 cell counting.

635

636 **Immunostainings**

637 Adult fruit-fly female brains were dissected (in PBS), fixed (in 4% para-formaldehyde, room temperature,
638 20-30min) and stained following standard protocols. Primary antibodies and their dilutions were as follows:
639 Mouse anti-Brp (nc82) 1:10 (DSHB); Rabbit anti-GFP 1:250 (Thermofisher); Mouse anti-GFP 1:250
640 (Thermofisher); Chicken anti-GFP 1:500 (Aves); Rabbit anti-FLAG 1:50 (Sigma); Mouse anti-V5 1:50
641 (Invitrogen); Chicken anti-HA 1:50 (Aves); Rabbit anti-VGlut 1:500 (gift of Hermann); Mouse anti-TH 1:250
642 (Immunostar); Rabbit anti-TH 1:250 (Novus Biologicals); Rabbit anti-DsRed 1:250 (Clontek); Mouse anti-
643 ChAT4B1 1:250 (DSHB); Rabbit anti-5-HT 1:500 (Immunostar); Rabbit Anti-DCP-1 1:250 (Cell Signalling).
644 Seconday antibodies were all used at 1:500 and all were from Thermofisher: Alexa Flour 488 Goat anti-
645 mouse, Alexa Flour 488 donkey anti-rabbit, Alexa Flour 488 Goat anti-rabbit (Fab')2, Alexa Flour 488 Goat
646 anti-chicken, Alexa Four 546 Goat anti-rabbit, Alexa Four 546 Goat anti-mouse, Alex Four 647 Goat anti-
647 rabbit, Alex Four 647 Goat anti-mouse.

648

649 **Microscopy and Imaging**

650 **Laser scanning confocal microscopy.** Stacks of microscopy images were acquired using laser scanning
651 confocal microscopy with either Zeiss LSM710, 900 or Leica SP8. Brains were scanned with a resolution of
652 1024x1024, with Leica SP8 20x oil objective and 1 mm step for whole brain and DCP-1 stainings, 40x oil
653 objective and 1 mm step for central brain. Resolution of 1024x512 was used for analysing PAM clusters
654 with 0.96 mm step for cell counting; 0.5 mm step for neuronal morphology; and 63x oil objective with
655 0.5mm step for neuronal connections. Acquisition speed in Leica SP8 was 400Hz, with no line averaging.
656 Resolution of 3072x3072 was used for single image analysis of synapses, using either Leica SP8 or Zeiss
657 LSM900 and Airyscan acquisition with 40x water objective speed 6, and average 4, or with 1024x512, with
658 40x oil lens 2x zoom and 0.35mm step. TH counting in PAM were scanned with Zeiss 710 with a resolution
659 1024x1024, 40x oil objective, step 1 mm, speed 8. Zeiss LSM900 Airyscan with a resolution of 1024x1024,
660 40x water objective, speed 7, 0.7 zoom and 0.31µm step size was used for acquisition of optical sections of
661 synapses in PAM neurons.

662 **Optogenetics and Epac1 FRET 2-photon imaging**

663 To test whether DNT-2 neurons can respond to dopamine via the Dop2R inhibitory receptor, we used the
664 cAMP sensor Epac1 and 2-photon confocal microscopy. Epac1 is FRET probe, whereby data are acquired
665 from CFP and YFP emission and lower YFP/CFP ratio reveals higher cAMP levels. DNT-2Gal4 flies were
666 crossed to *UAS-CsChrimson UAS Epac1* flies, to stimulate DNT-2 neurons and detect cAMP levels in DNT2
667 neurons. 1-3 day-old *DNT2Gal4>UASCsChrimson, UAS Epac1* flies were collected and separated in two
668 groups. Flies bearing *DNT2Gal4 UASCsChrimson UAS Epac1 UASDop2RRNAi* were fed on 50µM all-trans
669 retinal food for at least 3 days prior to imaging and kept in constant darkness prior to the experiment.

670 Optogenetic stimulation of fly brains expressing CsChrimson in DNT-2 neurons was carried out
671 using a sapphire 588nm laser, in a 2-photon confocal microscope. For acquisition of YFP and CFP data from
672 Epac1 samples, a FV30-FYC filter was applied, using a 925nm laser for both YFP and CFP imaging. The
673 stimulation laser was targeted onto DNT-2 neuron projections in SMP region for 20s. Acquisition ROI was at

674 DNT-2A cell bodies with a frame rate of around 10Hz. The first acquisition started 10s before the 20s
675 stimulation and consequential acquisition was done every 30s for 10 cycles.
676 Image analysis of Epac data was carried out using ImageJ. The two channels (YFP and CFP) were
677 separated, and the ratio of YFP/CFP for each pixel was calculated using the ImageJ>Image Calculator by
678 diving YFP channel by CFP channel. The obtained result of YFP/CFP ratio was saved and the mean ratio of
679 YFP/CFP in the ROI was calculated for each time point and 11 time points were used. The 11 values
680 represent the ratio of YFP/CFP change in the cell body upon stimulation, with 30s interval and repeated 10
681 times.
682 **Cell counting:** To count cells labelled with nuclear reporters (e.g. Histone-YFP, nls-tdTomato) and Dcp-1+
683 cells, where signal is of high intensity, contrast and sphericity, we adapted the DeadEasy Central Brain
684 ImageJ plug-in(Li et al. 2020) for automatic cell counting in adult brains. DeadEasy plug-ins automatically
685 identify and count cells labelled with nuclear reporters in 3D stacks of confocal image in the nervous
686 system of embryos (Forero et al. 2010a, Forero et al. 2010b), larvae(Kato et al. 2011, Forero et al. 2012,
687 Losada-Perez et al. 2016, Harrison et al. 2021) and adult(Li et al. 2020) *Drosophila*. DeadEasy plug-ins are
688 accurate at counting cells sparsely labelled with nuclear markers, and importantly, treat all genotypes
689 objectively and equally yielding reliable data. Here, adult brains expressing Histone-YFP or nls-td-tomato
690 reporters were dissected, fixed and scanned without staining them. DeadEasy Central Brain was used with
691 threshold set to 75.
692 To count the TH labelled PAMs, where both the signal and the labelled-cell shape are more
693 irregular, we used assisted manual cell counting using two methods. First, we developed a plug-in called
694 DeadEasy DAN as follows. A median filter was used to reduce Poison noise, without having large losses at
695 the edges. Then, a 3D morphological closing was performed. Next, all very dark pixels were assigned a value
696 of zero. To mark each cell, each chasm in the image was found using a 3D extended h-minimal transform.
697 As more than one local minimum can be found within each cell, which would result in counting a cell
698 multiple times, a 3D inverse dome detection was performed, and then labelled. Thus, each inverse dome
699 was used as a seed to identify each cell. Once the seeds were obtained, a 3D watershed transformation was

700 performed to recover the shape of the cells. The, we ran DeadEasy DAN on our raw data, to obtain a results
701 stack of images and formed a merged stack between the raw and result stacks, to manually add any missing
702 cells. This assisted cell counting method was effective at producing accurate cell counts with less labour
703 and time than conventional manual counting and worked well for some genotypes (Figure 3D). However, it
704 was less effective with RNAi knock-down genotypes, where the signal can be less intense, for which TH+
705 cells were counted manually, assisted by the ImageJ cell counter instead.
706 **Dendrite analysis with Imaris:** To analyze dendritic complexity, image data were processed with Imaris
707 using the "Filament Autodetect" function with the default algorithm and autopatch function. Setting of the
708 threshold was consistent within the same experiment: the largest or smallest diameter of the dendrite,
709 same threshold for background substation, local contrast. Number of dendritic branches, dendritic
710 segments, dendritic branch points and dendritic terminal points were collected to compare the difference
711 between the groups.
712 **Vesicles, synapses and PSD analysis with Imaris:** To analyse the number and volume of Homer-GCaMP
713 GFP+ post-synaptic densities (PSD), Syt-GCaMP GFP+ presynaptic sites and DNT-2FLGFP+ vesicles, optical
714 section images of confocal stacks through the brain were processed with the Imaris Spot function. Setting
715 of the threshold was consistent across genotypes.
716
717 **Behaviour**
718 **1. Startle induced negative geotaxis Assay** was carried out as described in (Sun et al. 2018). Groups of
719 approximately 10 male flies of the same genotype were placed in a fresh tube one night before the test,
720 after which flies were transferred to a column formed with two empty tubes 15cm long and 2cm and then
721 habituated for 30mins. Columns were tapped 3-4 times, flies fell to the bottom and then climbed upwards.
722 Multiple rounds of testing were performed 3-7 times in a row per column. The process was filmed and films
723 were analysed. Flies were scored during the first 15s after the tapping, and those that climbed above 13cm
724 and those that climbed below 2cm were counted separately. Results given are mean ± SEM of the scores
725 obtained with ten groups of flies per genotype. The performance index (PI) is defined as $1/2[(n_{tot} + n_{top} -$

726 $n_{bot})/n_{tot}]$, where n_{tot}, n_{top}, and n_{bot} are the total number of flies, the number of flies at the top, and
727 the number of flies at the bottom, respectively. The assay was carried out at 25°C, 55% humidity. Flies with
728 tubGal80^{ts} to conditionally overexpress or knock-down were shifted from 18 to 30°at eclosion and kept for
729 5 days at 30°C to induce Gal4. Experiments were carried in an environmental chamber at 31°C, 60%
730 humidity or in a humidity and temperature-controlled behaviour lab always kept at 25°C.
731 **2. Spontaneous Locomotion in an open arena:** Male flies of each genotype were collected and kept in groups
732 of 10-20 flies, in vials containing fresh fly food for 5-9 days. Before filming, three male flies from one genotype
733 were transferred into a 24 mm well of a multi-well plate using an aspirator and habituated for 15 – 20 mins.
734 The multi-well plate with transparent lid and bottom was placed on a white LED light pad (XIAOSTAR Light
735 Box) and either inside a light-shielding black box (PULUZ, 40*40*40cm) in a room with constant temperature
736 (25°C) and humidity (55%) to maintain stable environmental conditions (Figure 7D), or inside a temperature
737 controlled environmental chamber at 18°C or 30°C (Figure 7E,F,) . The locomotion behaviour of freely-moving
738 flies was filmed with a camera (Panasonic, HC-V260) in the morning from ZT1-ZT4 and for 10 min at a frame-
739 rate of 25 fps. The 10-min videos were trimmed (from 00:02:00 to 00:07:00) to 5-min videos for analysis using
740 Flytracker software(Eyjolfsdottir et al. 2014). For the *DNT-2* mutants and over-expression of Toll-6^{CY}
741 experiments, flies were bred and tested at 25 °C. To test over-expression of *DNT-2* with *tubGAL80^{ts}; DNT2-*
742 *Gal4>UAS-DNT-2FL*, flies were raised at 18°C until eclosion, and controls were kept and tested at 18°C; test
743 groups were transferred directly after eclosion to 30°C for 5 days and were tested in an environmental
744 chamber kept at 30°C, 60%. For thermo-genetic activation of DNT2 neurons using TrpA1 (DNT-
745 2GAL4>UASTrpA1), flies were bred at 18°C and kept at 18°C for 7-9 days post-eclosion. Following habituation
746 at 18°c for 20 mins in the multi-well plates, they were transferred to the 30°C chamber 10 mins before filming
747 to activate TrpA1 and then filmed for the following 10 minutes. Fly locomotion activity was tracked using
748 FlyTracker and calculated (distance and speed) in Matlab(Eyjolfsdottir et al. 2014) using the raw data
749 generated from the tracking procedure. The "walking distance" was calculated as the sum of the distance
750 flies moved and the "walking speed" was the speed of flies only when they were walking, and it was
751 calculated using only frames where flies moved above 4 mm/s (which corresponds to two body lengths).

752 **3. Appetitive long term memory test:** Appetitive long-term memory was tested as described in Krashes and
753 Waddell(Krashes and Waddell 2011). The two conditioning odours used were isoamyl acetate, Sigma-Aldrich
754 #24900822, 6mL in 8mL mineral oil (Sigma-Aldrich #330760) and 4-methylcyclohexanol (Sigma-Aldrich #
755 153095, 10mL in 8mL mineral oil). Groups of 80-120 mixed sex flies were starved in a 1% agar tube filled with
756 a damp 20 x 60 mm piece of filter paper for 18-20 hour before conditioning. During conditioning training,
757 one odorant was presented with a dry filter paper (unconditioned odour, CS-) for 2 minutes, before a 30
758 second break, and presentation of a second odorant with filter paper coated with dry sucrose (conditioned
759 odour, CS+). The test was repeated pairing the other odorant with sucrose, with a different group of flies to
760 form one replicate. After training, flies were transferred back to agar tubes for testing 24 hours later.
761 Performance index (PI) was calculated in the same way as in Krashes and Waddell(Krashes and Waddell
762 2011), as the number of flies approaching the conditioned odour minus the number of flies going in the
763 opposite direction, divided by the total number of flies. A single PI values is the average score from the test
764 with the reverse conditioning odour combination. Groups for which the total number of flies among both
765 odorants was below 15 were discarded. For the *DNT-2* over-expression experiments with *tubGAL80^{ts}; DNT-*
766 *2>DNT-2FL,* flies were raised at 18°C until 7-9 days post-eclosion. They were then either transferred to and
767 maintained at 23°C (controls) or 30°C for 18-20h starvation, training, and up to testing 24h later.
768 **Statistical analysis:** Statistical analyses were carried out using Graph-Pad Prism. Confidence interval was
769 95%, setting significance at $p<0.05$. Chi-square tests were carried out when comparing categorical data.
770 Numerical data were tested first for their type of distributions. If data were distributed normally, unpaired
771 Student t-tests were used to compare means between two groups and One Way ANOVA or Welch ANOVA
772 for larger groups, followed by post-doc Dunnett test for multiple comparisons to a fixed control. Two Way
773 ANOVA was used when comparisons to two variables were made. If data were not normally distributed,
774 non-parametric Mann-Whitney U-test for 2 two group comparisons and Kruskal Wallis ANOVA for larger
775 groups, followed by post-hoc Dunn's multiple comparisons test to a fixed control. Statistical details
776 including full genotypes, sample sizes, tests and p values are provided in Supplementary Table S2.
777

REFERENCES

Adel, M. and L. C. Griffith (2021). "The Role of Dopamine in Associative Learning in Drosophila: An Updated Unified Model." *Neurosci Bull* **37**(6): 831-852.

Adhikarla, S. V., N. K. Jha, V. K. Goswami, A. Sharma, A. Bhardwaj, A. Dey, C. Villa, Y. Kumar and S. K. Jha (2021). "TLR-Mediated Signal Transduction and Neurodegenerative Disorders." *Brain Sci* **11**(11).

Anthoney, N., I. Foldi and A. Hidalgo (2018). "Toll and Toll-like receptor signalling in development." *Development* **145**(9).

Arikkath, J. (2012). "Molecular mechanisms of dendrite morphogenesis." *Front Cell Neurosci* **6**: 61.

Arnot, C. J., N. J. Gay and M. Gangloff (2010). "Molecular mechanism that induces activation of Spatzle, the ligand for the Drosophila Toll receptor." *J Biol Chem* **285**(25): 19502-19509.

Aso, Y., D. Hattori, Y. Yu, R. M. Johnston, N. A. Iyer, T. T. Ngo, H. Dionne, L. F. Abbott, R. Axel, H. Tanimoto and G. M. Rubin (2014a). "The neuronal architecture of the mushroom body provides a logic for associative learning." *Elife* **3**: e04577.

Aso, Y., A. Herb, M. Ogueta, I. Siwanowicz, T. Templier, A. B. Friedrich, K. Ito, H. Scholz and H. Tanimoto (2012). "Three dopamine pathways induce aversive odor memories with different stability." *PLoS Genet* **8**(7): e1002768.

Aso, Y., D. Sitaraman, T. Ichinose, K. R. Kaun, K. Vogt, G. Belliart-Guerin, P. Y. Placais, A. A. Robie, N. Yamagata, C. Schnaitmann, W. J. Rowell, R. M. Johnston, T. T. Ngo, N. Chen, W. Korff, M. N. Nitabach, U. Heberlein, T. Preat, K. M. Branson, H. Tanimoto and G. M. Rubin (2014b). "Mushroom body output neurons encode valence and guide memory-based action selection in Drosophila." *Elife* **3**: e04580.

Baltruschat, L., L. Prisco, P. Ranft, J. S. Lauritzen, A. Fiala, D. D. Bock and G. Tavosanis (2021). "Circuit reorganization in the Drosophila mushroom body calyx accompanies memory consolidation." *Cell Rep* **34**(11): 108871.

Barth, M. and M. Heisenberg (1997). "Vision affects mushroom bodies and central complex in Drosophila melanogaster." *Learn Mem* **4**(2): 219-229.

Barth, M., H. V. Hirsch, I. A. Meinertzhagen and M. Heisenberg (1997). "Experience-dependent developmental plasticity in the optic lobe of Drosophila melanogaster." *J Neurosci* **17**(4): 1493-1504.

Berton, O., C. A. McClung, R. J. Dileone, V. Krishnan, W. Renthal, S. J. Russo, D. Graham, N. M. Tsankova, C. A. Bolanos, M. Rios, L. M. Monteggia, D. W. Self and E. J. Nestler (2006). "Essential role of BDNF in the mesolimbic dopamine pathway in social defeat stress." *Science* **311**(5762): 864-868.

Bharmauria, V., A. Ouelhazi, R. Lussiez and S. Molotchnikoff (2022). "Adaptation-induced plasticity in the sensory cortex." *J Neurophysiol* **128**(4): 946-962.

Blochl, A. and C. Sirrenberg (1996). "Neurotrophins stimulate the release of dopamine from rat mesencephalic neurons via Trk and p75Lntr receptors." *J Biol Chem* **271**(35): 21100-21107.

Bolus, H., K. Crocker, G. Boekhoff-Falk and S. Chtarbanova (2020). "Modeling Neurodegenerative Disorders in Drosophila melanogaster." *Int J Mol Sci* **21**(9).

Boto, T., T. Louis, K. Jindachomthong, K. Jalink and S. M. Tomchik (2014). "Dopaminergic modulation of cAMP drives nonlinear plasticity across the Drosophila mushroom body lobes." *Curr Biol* **24**(8): 822-831.

Boto, T., A. Stahl and S. M. Tomchik (2020). "Cellular and circuit mechanisms of olfactory associative learning in Drosophila." *J Neurogenet* **34**(1): 36-46.

Bushey, D., G. Tononi and C. Cirelli (2011). "Sleep and synaptic homeostasis: structural evidence in Drosophila." *Science* **332**(6037): 1576-1581.

Cachero, S., M. Gkantia, A. S. Bates, S. Frechter, L. Blackie, A. McCarthy, B. Sutcliffe, A. Strano, Y. Aso and G. S. X. E. Jefferis (2020). "BAcTrace a new tool for retrograde tracing of neuronal circuit." *Nature Methods* **17**: 1254-1261.

Carim-Todd, L., K. G. Bath, G. Fulgenzi, S. Yanpallewar, D. Jing, C. A. Barrick, J. Becker, H. Buckley, S. G. Dorsey, F. S. Lee and L. Tessarollo (2009). "Endogenous truncated TrkB.T1 receptor regulates neuronal complexity and TrkB kinase receptor function in vivo." *J Neurosci* **29**(3): 678-685.

Casarotto, P. C., M. Girych, S. M. Fred, V. Kovaleva, R. Moliner, G. Enkavi, C. Biojone, C. Cannarozzo, M. P. Sahu, K. Kaurinkoski, C. A. Brunello, A. Steinzeig, F. Winkel, S. Patil, S. Vestring, T. Serchov, C. Diniz, L. Laukkanen, I. Cardon, H. Antila, T. Rog, T. P. Piepponen, C. R. Bramham, C. Normann, S. E. Lauri, M. Saarma, I. Vattulainen and E. Castren (2021). "Antidepressant drugs act by directly binding to TRKB neurotrophin receptors." *Cell* **184**(5): 1299-1313 e1219.

Castren, E. and L. Monteggia (2021). "Brain-Derived Neurotrophic Factor Signaling in Depression and Antidepressant Action." *Biol Psychiatry*.

Chan, R. F., G. Turecki, A. A. Shabalin, J. Guintivano, M. Zhao, L. Y. Xie, G. van Grootheest, Z. A. Kaminsky, B. Dean, B. Penninx, K. A. Aberg and E. van den Oord (2020). "Cell Type-Specific Methylome-wide Association Studies Implicate Neurotrophin and Innate Immune Signaling in Major Depressive Disorder." *Biol Psychiatry* **87**(5): 431-442.

Chen, C. C. and J. C. Brumberg (2021). "Sensory Experience as a Regulator of Structural Plasticity in the Developing Whisker-to-Barrel System." *Frontiers in Cellular Neuroscience* **15**.

Chen, C. C., J. K. Wu, H. W. Lin, T. P. Pai, T. F. Fu, C. L. Wu, T. Tully and A. S. Chiang (2012). "Visualizing long-term memory formation in two neurons of the Drosophila brain." *Science* **335**(6069): 678-685.

Chen, C. Y., Y. C. Shih, Y. F. Hung and Y. P. Hsueh (2019). "Beyond defense: regulation of neuronal morphogenesis and brain functions via Toll-like receptors." *J Biomed Sci* **26**(1): 90.

Cheng, L. K., Y. H. Chiu, Y. C. Lin, W. C. Li, T. Y. Hong, C. J. Yang, C. H. Shih, T. C. Yeh, W. I. Tseng, H. Y. Yu, J. C. Hsieh and L. F. Chen (2022). "Long-term musical training induces white matter plasticity in emotion and language networks." *Hum Brain Mapp*.

Coban, B., H. Poppinga, E. Y. Rachad, B. Geurten, D. Vasmer, F. J. Rodriguez Jimenez, Y. Gadgil, S. H. Deimel, I. Alyagor, O. Schuldiner, I. C. Grunwald Kadow, T. D. Riemensperger, A. Widmann and A.

850 Fiala (2024). "The caloric value of food intake structurally adjusts a neuronal mushroom body circuit
851 mediating olfactory learning in Drosophila." *Learn Mem* **31**(5).

852 Costa, M., J. D. Manton, A. D. Ostrovsky, S. Prohaska and G. S. Jefferis (2016). "NBLAST: Rapid,
853 Sensitive Comparison of Neuronal Structure and Construction of Neuron Family Databases." *Neuron*
854 **91**(2): 293-311.

855 Cotman, C. W. and N. C. Berchtold (2002). "Exercise: a behavioral intervention to enhance brain
856 health and plasticity." *Trends Neurosci* **25**(6): 295-301.

857 Croset, V., C. D. Treiber and S. Waddell (2018). "Cellular diversity in the Drosophila midbrain
858 revealed by single-cell transcriptomics." *Elife* **7**.

859 DeLotto, Y. and R. DeLotto (1998). "Proteolytic processing of the Drosophila Spatzle protein by
860 easter generates a dimeric NGF-like molecule with ventralising activity." *Mech Dev* **72**(1-2): 141-
861 148.

862 Devaud, J. M., A. Acebes and A. Ferrus (2001). "Odor exposure causes central adaptation and
863 morphological changes in selected olfactory glomeruli in Drosophila." *J Neurosci* **21**(16): 6274-6282.

864 Duhart, J. M., A. Herrero, G. de la Cruz, J. I. Ispizua, N. Pirez and M. F. Ceriani (2020). "Circadian
865 Structural Plasticity Drives Remodeling of E Cell Output." *Curr Biol* **30**(24): 5040-5048 e5045.

866 Ernst, C., V. Deleva, X. Deng, A. Sequeira, A. Pomarenski, T. Klempan, N. Ernst, R. Quirion, A. Gratton,
867 M. Szyf and G. Turecki (2009). "Alternative splicing, methylation state, and expression profile of
868 tropomyosin-related kinase B in the frontal cortex of suicide completers." *Arch Gen Psychiatry* **66**(1):
869 22-32.

870 Eyjolfsdottir, E., S. Branson, X. P. Burgos-Artizzu, E. D. Hoopfer, J. Schor, D. J. Anderson and P. Perona
871 (2014). Detecting Social Actions of Fruit Flies, Cham, Springer International Publishing.

872 Feany, M. B. and W. W. Bender (2000). "A Drosophila model of Parkinson's disease." *Nature*
873 **404**(6776): 394-398.

874 Feldman, D. E. and M. Brecht (2005). "Map plasticity in somatosensory cortex." *Science* **310**(5749):
875 810-815.

876 Fenner, B. M. (2012). "Truncated TrkB: beyond a dominant negative receptor." *Cytokine Growth*
877 *Factor Rev* **23**(1-2): 15-24.

878 Fernandez, M. P., J. Berni and M. F. Ceriani (2008). "Circadian remodeling of neuronal circuits
879 involved in rhythmic behavior." *PLoS Biol* **6**(3): e69.

880 Ferrer, I., C. Marin, M. J. Rey, T. Ribalta, E. Goutan, R. Blanco, E. Tolosa and E. Marti (1999). "BDNF
881 and full-length and truncated TrkB expression in Alzheimer disease. Implications in therapeutic
882 strategies." *J Neuropathol Exp Neurol* **58**(7): 729-739.

883 Figueroa-Hall, L. K., M. P. Paulus and J. Savitz (2020). "Toll-Like Receptor Signaling in Depression."
884 *Psychoneuroendocrinology* **121**: 104843.

885 Foldi, I., N. Anthoney, N. Harrison, M. Gangloff, B. Verstak, M. P. Nallasivan, S. AlAhmed, B. Zhu, M.
886 Phizacklea, M. Losada-Perez, M. Moreira, N. J. Gay and A. Hidalgo (2017). "Three-tier regulation of
887 cell number plasticity by neurotrophins and Tolls in Drosophila." *J Cell Biol* **216**(5): 1421-1438.

888 Forero, M. G., K. Kato and A. Hidalgo (2012). "Automatic cell counting in vivo in the larval nervous
889 system of Drosophila." *J Microsc* **246**(2): 202-212.

890 Forero, M. G., A. R. Learte, S. Cartwright and A. Hidalgo (2010a). "DeadEasy Mito-Glia: automatic
891 counting of mitotic cells and glial cells in Drosophila." *PLoS One* **5**(5): e10557.

892 Forero, M. G., J. A. Pennack and A. Hidalgo (2010b). "DeadEasy neurons: automatic counting of HB9
893 neuronal nuclei in Drosophila." *Cytometry A* **77**(4): 371-378.

894 Forero, M. G., J. A. Pennack, A. R. Learte and A. Hidalgo (2009). "DeadEasy caspase: automatic
895 counting of apoptotic cells in Drosophila." *PLoS One* **4**(5): e5441.

896 Forrest, M. P., E. Parnell and P. Penzes (2018). "Dendritic structural plasticity and neuropsychiatric
897 disease." *Nat Rev Neurosci* **19**(4): 215-234.

898 Fryer, R. H., D. R. Kaplan, S. C. Feinstein, M. J. Radeke, D. R. Grayson and L. F. Kromer (1996).
899 "Developmental and mature expression of full-length and truncated TrkB receptors in the rat
900 forebrain." *J Comp Neurol* **374**(1): 21-40.

901 Fuentes-Medel, Y., M. A. Logan, J. Ashley, B. Ataman, V. Budnik and M. R. Freeman (2009). "Glia and
902 muscle sculpt neuromuscular arbors by engulfing destabilized synaptic boutons and shed
903 presynaptic debris." *PLoS Biol* **7**(8): e1000184.

904 Gage, F. H. (2019). "Adult neurogenesis in mammals." *Science* **364**(6443): 827-828.

905 Garrett, M. E., X. J. Qin, D. Mehta, M. F. Dennis, C. E. Marx, G. A. Grant, V. A. M.-A. M. Workgroup,
906 P. Initiative, Injury, C. Traumatic Stress Clinical, P. G. Psychiatric Genomics Consortium, M. B. Stein,
907 N. A. Kimbrel, J. C. Beckham, M. A. Hauser and A. E. Ashley-Koch (2021). "Gene Expression Analysis
908 in Three Posttraumatic Stress Disorder Cohorts Implicates Inflammation and Innate Immunity
909 Pathways and Uncovers Shared Genetic Risk With Major Depressive Disorder." *Front Neurosci* **15**:
910 678548.

911 Gay, N. J. and M. Gangloff (2007). "Structure and function of Toll receptors and their ligands." *Annu*
912 *Rev Biochem* **76**: 141-165.

913 Gorska-Andrzejak, J., A. Keller, T. Raabe, L. Kilianek and E. Pyza (2005). "Structural daily rhythms in
914 GFP-labelled neurons in the visual system of Drosophila melanogaster." *Photochem Photobiol Sci*
915 **4**(9): 721-726.

916 Guillin, O., J. Diaz, P. Carroll, N. Griffon, J. C. Schwartz and P. Sokoloff (2001). "BDNF controls
917 dopamine D3 receptor expression and triggers behavioural sensitization." *Nature* **411**(6833): 86-89.

918 Guven-Ozkan, T. and R. L. Davis (2014). "Functional neuroanatomy of Drosophila olfactory memory
919 formation." *Learn Mem* **21**(10): 519-526.

920 Harrison, N. J., E. Connolly, A. Gascon Gubieda, Z. Yang, B. Altenhein, M. Losada Perez, M. Moreira,
921 J. Sun and A. Hidalgo (2021). "Regenerative neurogenic response from glia requires insulin-driven
922 neuron-glia communication." *Elife* **10**.

923 Hearn, M. G., Y. Ren, E. W. McBride, I. Reveillaud, M. Beinborn and A. S. Kopin (2002). "A Drosophila
924 dopamine 2-like receptor: Molecular characterization and identification of multiple alternatively
925 spliced variants." *Proc Natl Acad Sci U S A* **99**(22): 14554-14559.

926 Heisenberg, M. (2003). "Mushroom body memoir: from maps to models." *Nat Rev Neurosci* **4**(4):
927 266-275.

928 Heisenberg, M., M. Heusipp and C. Wanke (1995). "Structural plasticity in the Drosophila brain." *J*
929 *Neurosci* **15**(3 Pt 1): 1951-1960.

930 Hepburn, L., T. K. Prajsnar, C. Klapholz, P. Moreno, C. A. Loynes, N. V. Ogryzko, K. Brown, M.
931 Schiebler, K. Hegyi, R. Antrobus, K. L. Hammond, J. Connolly, B. Ochoa, C. Bryant, M. Otto, B.
932 Surewaard, S. L. Seneviratne, D. M. Grogono, J. Cachat, T. Ny, A. Kaser, M. E. Torok, S. J. Peacock, M.
933 Holden, T. Blundell, L. Wang, P. Ligoxygakis, L. Minichiello, C. G. Woods, S. J. Foster, S. A. Renshaw
934 and R. A. Floto (2014). "Innate immunity. A Spaetzle-like role for nerve growth factor beta in
935 vertebrate immunity to Staphylococcus aureus." *Science* **346**(6209): 641-646.

936 Hoffmann, A., A. Funkner, P. Neumann, S. Juhnke, M. Walther, A. Schierhorn, U. Weininger, J.
937 Balbach, G. Reuter and M. T. Stubbs (2008a). "Biophysical characterization of refolded Drosophila
938 Spatzle, a cystine knot protein, reveals distinct properties of three isoforms." *J Biol Chem* **283**(47):
939 32598-32609.

940 Hoffmann, A., P. Neumann, A. Schierhorn and M. T. Stubbs (2008b). "Crystallization of Spatzle, a
941 cystine-knot protein involved in embryonic development and innate immunity in Drosophila
942 melanogaster." *Acta Crystallogr Sect F Struct Biol Cryst Commun* **64**(Pt 8): 707-710.

943 Holtmaat, A. and K. Svoboda (2009). "Experience-dependent structural synaptic plasticity in the
944 mammalian brain." *Nat Rev Neurosci* **10**(9): 647-658.

945 Horch, H. W. and L. C. Katz (2002). "BDNF release from single cells elicits local dendritic growth in
946 nearby neurons." *Nat Neurosci* **5**(11): 1177-1184.

947 Hu, X., Y. Yagi, T. Tanji, S. Zhou and Y. T. Ip (2004). "Multimerization and interaction of Toll and
948 Spatzle in Drosophila." *Proc Natl Acad Sci U S A* **101**(25): 9369-9374.

949 Hyman, C., M. Hofer, Y. A. Barde, M. Juhasz, G. D. Yancopoulos, S. P. Squinto and R. M. Lindsay
950 (1991). "BDNF is a neurotrophic factor for dopaminergic neurons of the substantia nigra." *Nature*
951 **350**(6315): 230-232.

952 Jenks, K. R., K. Tsimring, J. P. K. Ip, J. C. Zepeda and M. Sur (2021). "Heterosynaptic Plasticity and the
953 Experience-Dependent Refinement of Developing Neuronal Circuits." *Front Neural Circuits* **15**:
954 803401.

955 Kato, K., M. G. Forero, J. C. Fenton and A. Hidalgo (2011). "The glial regenerative response to central
956 nervous system injury is enabled by pros-notch and pros-NFkappaB feedback." *PLoS Biol* **9**(8):
957 e1001133.

958 Krashes, M. J. and S. Waddell (2008). "Rapid consolidation to a radish and protein synthesis-
959 dependent long-term memory after single-session appetitive olfactory conditioning in Drosophila."
960 *J Neurosci* **28**(12): 3103-3113.

961 Krashes, M. J. and S. Waddell (2011). "Drosophila appetitive olfactory conditioning." *Cold Spring*
962 *Harb Protoc* **2011**(5): pdb prot5609.

963 Kremer, M. C., F. Christiansen, F. Leiss, M. Paehler, S. Knapek, T. F. Andlauer, F. Forstner, P.
964 Kloppenburg, S. J. Sigrist and G. Tavosanis (2010). "Structural long-term changes at mushroom body
965 input synapses." *Curr Biol* **20**(21): 1938-1944.

966 Krishnan, V. and E. J. Nestler (2008). "The molecular neurobiology of depression." *Nature* **455**(7215):
967 894-902.

968 Kuner, R. and H. Flor (2016). "Structural plasticity and reorganisation in chronic pain." *Nat Rev*
969 *Neurosci* **18**(1): 20-30.

970 Lee, J. L., B. J. Everitt and K. L. Thomas (2004). "Independent cellular processes for hippocampal
971 memory consolidation and reconsolidation." *Science* **304**(5672): 839-843.

972 Leemhuis, E., L. De Gennaro and A. M. Pazzaglia (2019). "Disconnected Body Representation:
973 Neuroplasticity Following Spinal Cord Injury." *J Clin Med* **8**(12).

974 Levi-Montalcini, R., S. D. Skaper, R. Dal Toso, L. Petrelli and A. Leon (1996). "Nerve growth factor:
975 from neurotrophin to neurokine." *Trends Neurosci* **19**(11): 514-520.

976 Lewis, M., C. J. Arnot, H. Beeston, A. McCoy, A. E. Ashcroft, N. J. Gay and M. Gangloff (2013).
977 "Cytokine Spatzle binds to the Drosophila immunoreceptor Toll with a neurotrophin-like specificity
978 and couples receptor activation." *Proc Natl Acad Sci U S A* **110**(51): 20461-20466.

979 Li, G., M. G. Forero, J. S. Wentzell, I. Durmus, R. Wolf, N. C. Anthoney, M. Parker, R. Jiang, J.
980 Hasenauer, N. J. Strausfeld, M. Heisenberg and A. Hidalgo (2020). "A Toll-receptor map underlies
981 structural brain plasticity." *Elife* **9**.

982 Li, G. and A. Hidalgo (2021). "The Toll Route to Structural Brain Plasticity." *Front Physiol* **12**: 679766.

983 Linneweber, G. A., M. Andriatsilavo, S. B. Dutta, M. Bengochea, L. Hellbruegge, G. Liu, R. K. Ejsmont,
984 A. D. Straw, M. Wernet, P. R. Hiesinger and B. A. Hassan (2020). "A neurodevelopmental origin of
985 behavioral individuality in the Drosophila visual system." *Science* **367**(6482): 1112-1119.

986 Liu, C., P. Y. Placais, N. Yamagata, B. D. Pfeiffer, Y. Aso, A. B. Friedrich, I. Siwanowicz, G. M. Rubin, T.
987 Preat and H. Tanimoto (2012). "A subset of dopamine neurons signals reward for odour memory in
988 Drosophila." *Nature* **488**(7412): 512-516.

989 Losada-Perez, M., N. Harrison and A. Hidalgo (2016). "Molecular mechanism of central nervous
990 system repair by the Drosophila NG2 homologue kon-tiki." *J Cell Biol* **214**(5): 587-601.

991 Lu, B., G. Nagappan, X. Guan, P. J. Nathan and P. Wren (2013). "BDNF-based synaptic repair as a
992 disease-modifying strategy for neurodegenerative diseases." *Nat Rev Neurosci* **14**(6): 401-416.

993 Lu, B., P. T. Pang and N. H. Woo (2005). "The yin and yang of neurotrophin action." *Nat Rev Neurosci*
994 **6**(8): 603-614.

995 Ma, Y., J. Li, I. Chiu, Y. Wang, J. A. Sloane, J. Lu, B. Kosaras, R. L. Sidman, J. J. Volpe and T. Vartanian
996 (2006). "Toll-like receptor 8 functions as a negative regulator of neurite outgrowth and inducer of
997 neuronal apoptosis." *J Cell Biol* **175**(2): 209-215.

998 MacLaren, C. M., T. A. Evans, D. Alvarado and J. B. Duffy (2004). "Comparative analysis of the Kekkon
999 molecules, related members of the LIG superfamily." *Dev Genes Evol* **214**(7): 360-366.

1000 Maguire, E. A., D. G. Gadian, I. S. Johnsrude, C. D. Good, J. Ashburner, R. S. Frackowiak and C. D.
1001 Frith (2000). "Navigation-related structural change in the hippocampi of taxi drivers." *Proc Natl Acad*
1002 *Sci U S A* **97**(8): 4398-4403.

1003 Mandai, K., T. Guo, C. St Hillaire, J. S. Meabon, K. C. Kanning, M. Bothwell and D. D. Ginty (2009).
1004 "LIG family receptor tyrosine kinase-associated proteins modulate growth factor signals during
1005 neural development." *Neuron* **63**(5): 614-627.

1006 Martinowich, K., H. Manji and B. Lu (2007). "New insights into BDNF function in depression and
1007 anxiety." *Nat Neurosci* **10**(9): 1089-1093.

1008 Mayseless, O., D. S. Berns, X. M. Yu, T. Riemensperger, A. Fiala and O. Schuldiner (2018).
1009 "Developmental Coordination during Olfactory Circuit Remodeling in Drosophila." *Neuron* **99**(6):
1010 1204-1215 e1205.

1011 McIlroy, G., I. Foldi, J. Aurikko, J. S. Wentzell, M. A. Lim, J. C. Fenton, N. J. Gay and A. Hidalgo (2013).
1012 "Toll-6 and Toll-7 function as neurotrophin receptors in the Drosophila melanogaster CNS." *Nat*
1013 *Neurosci* **16**(9): 1248-1256.

1014 McLaughlin, C. N., I. V. Nechipurenko, N. Liu and H. T. Broihier (2016). "A Toll receptor-FoxO pathway
1015 represses Pavarotti/MKLP1 to promote microtubule dynamics in motoneurons." *J Cell Biol* **214**(4):
1016 459-474.

1017 McLaughlin, C. N., J. J. Perry-Richardson, J. C. Coutinho-Budd and H. T. Broihier (2019). "Dying
1018 Neurons Utilize Innate Immune Signaling to Prime Glia for Phagocytosis during Development." *Dev*
1019 *Cell* **48**(4): 506-522 e506.

1020 Mehta, D., J. Voisey, D. Bruenig, W. Harvey, C. P. Morris, B. Lawford and R. M. Young (2018).
1021 "Transcriptome analysis reveals novel genes and immune networks dysregulated in veterans with
1022 PTSD." *Brain Behav Immun* **74**: 133-142.

1023 Meyer, S. N., M. Amoyel, C. Bergantinos, C. de la Cova, C. Schertel, K. Basler and L. A. Johnston
1024 (2014). "An ancient defense system eliminates unfit cells from developing tissues during cell
1025 competition." *Science* **346**(6214): 1258236.

1026 Minichiello, L. (2009). "TrkB signalling pathways in LTP and learning." *Nat Rev Neurosci* **10**(12): 850-
1027 860.

1028 Nern, A., B. D. Pfeiffer and G. M. Rubin (2015). "Optimized tools for multicolor stochastic labeling
1029 reveal diverse stereotyped cell arrangements in the fly visual system." *Proc Natl Acad Sci U S A*
1030 **112**(22): E2967-2976.

1031 Neve, K. A., J. K. Seamans and H. Trantham-Davidson (2004). "Dopamine receptor signaling." *J*
1032 *Recept Signal Transduct Res* **24**(3): 165-205.

1033 Ohira, K. and M. Hayashi (2009). "A new aspect of the TrkB signaling pathway in neural plasticity."
1034 *Curr Neuropharmacol* **7**(4): 276-285.

1035 Ohira, K., K. J. Homma, H. Hirai, S. Nakamura and M. Hayashi (2006). "TrkB-T1 regulates the RhoA
1036 signaling and actin cytoskeleton in glioma cells." *Biochem Biophys Res Commun* **342**(3): 867-874.

1037 Okun, E., K. Griffioen, B. Barak, N. J. Roberts, K. Castro, M. A. Pita, A. Cheng, M. R. Mughal, R. Wan,
1038 U. Ashery and M. P. Mattson (2010). "Toll-like receptor 3 inhibits memory retention and constrains
1039 adult hippocampal neurogenesis." *Proc Natl Acad Sci U S A* **107**(35): 15625-15630.

1040 Okun, E., K. J. Griffioen and M. P. Mattson (2011). "Toll-like receptor signaling in neural plasticity
1041 and disease." *Trends Neurosci* **34**(5): 269-281.

1042 Pare, A. C., A. Vichas, C. T. Fincher, Z. Mirman, D. L. Farrell, A. Mainieri and J. A. Zallen (2014). "A
1043 positional Toll receptor code directs convergent extension in Drosophila." *Nature* **515**(7528): 523-
1044 527.

1045 Park, H. and M. M. Poo (2013). "Neurotrophin regulation of neural circuit development and
1046 function." *Nat Rev Neurosci* **14**(1): 7-23.

1047 Patel, V., A. M. Patel and J. J. McArdle (2016). "Synaptic abnormalities of mice lacking toll-like
1048 receptor (TLR)-9." *Neuroscience* **324**: 1-10.

1049 Pech, U., N. H. Revelo, K. J. Seitz, S. O. Rizzoli and A. Fiala (2015). "Optical dissection of experience-
1050 dependent pre- and postsynaptic plasticity in the Drosophila brain." *Cell Rep* **10**(12): 2083-2095.

1051 Placais, P. Y., S. Trannoy, G. Isabel, Y. Aso, I. Siwanowicz, G. Belliart-Guerin, P. Vernier, S. Birman, H.
1052 Tanimoto and T. Preat (2012). "Slow oscillations in two pairs of dopaminergic neurons gate long-
1053 term memory formation in Drosophila." *Nat Neurosci* **15**(4): 592-599.

1054 Poo, M. M. (2001). "Neurotrophins as synaptic modulators." *Nat Rev Neurosci* **2**(1): 24-32.

1055 Riemensperger, T., G. Isabel, H. Coulom, K. Neuser, L. Seugnet, K. Kume, M. Iche-Torres, M. Cassar,
1056 R. Strauss, T. Preat, J. Hirsh and S. Birman (2011). "Behavioral consequences of dopamine deficiency
1057 in the Drosophila central nervous system." *Proc Natl Acad Sci U S A* **108**(2): 834-839.

1058 Riemensperger, T., A. R. Issa, U. Pech, H. Coulom, M. V. Nguyen, M. Cassar, M. Jacquet, A. Fiala and
1059 S. Birman (2013). "A single dopamine pathway underlies progressive locomotor deficits in a
1060 Drosophila model of Parkinson disease." *Cell Rep* **5**(4): 952-960.

1061 Rolls, A., R. Shechter, A. London, Y. Ziv, A. Ronen, R. Levy and M. Schwartz (2007). "Toll-like receptors
1062 modulate adult hippocampal neurogenesis." *Nat Cell Biol* **9**(9): 1081-1088.

1063 Sachse, S., E. Rueckert, A. Keller, R. Okada, N. K. Tanaka, K. Ito and L. B. Vosshall (2007). "Activity-
1064 dependent plasticity in an olfactory circuit." *Neuron* **56**(5): 838-850.

1065 Sahu, M. P., Y. Pazos-Boubeta, C. Pajanoja, S. Rozov, P. Panula and E. Castren (2019). "Neurotrophin
1066 receptor Ntrk2b function in the maintenance of dopamine and serotonin neurons in zebrafish." *Sci*
1067 *Rep* **9**(1): 2036.

1068 Shafer, O. T., D. J. Kim, R. Dunbar-Yaffe, V. O. Nikolaev, M. J. Lohse and P. H. Taghert (2008).
1069 "Widespread receptivity to neuropeptide PDF throughout the neuronal circadian clock network of
1070 Drosophila revealed by real-time cyclic AMP imaging." *Neuron* **58**(2): 223-237.

1071 Sharma, A. (2012). "Genome-wide expression analysis in epilepsy: a synthetic review." *Curr Top Med*
1072 *Chem* **12**(9): 1008-1032.

1073 Squillace, S. and D. Salvemini (2022). "Toll-like receptor-mediated neuroinflammation: relevance for
1074 cognitive dysfunctions." *Trends Pharmacol Sci* **43**(9): 726-739.

1075 Stoilov, P., E. Castren and S. Stamm (2002). "Analysis of the human TrkB gene genomic organization
1076 reveals novel TrkB isoforms, unusual gene length, and splicing mechanism." *Biochem Biophys Res*
1077 *Commun* **290**(3): 1054-1065.

1078 Sugie, A., S. Hakeda-Suzuki, E. Suzuki, M. Silies, M. Shimozono, C. Mohl, T. Suzuki and G. Tavosanis
1079 (2015). "Molecular Remodeling of the Presynaptic Active Zone of Drosophila Photoreceptors via
1080 Activity-Dependent Feedback." *Neuron* **86**(3): 711-725.

1081 Sun, J., A. Q. Xu, J. Giraud, H. Poppinga, T. Riemensperger, A. Fiala and S. Birman (2018). "Neural
1082 Control of Startle-Induced Locomotion by the Mushroom Bodies and Associated Neurons in
1083 Drosophila." *Front Syst Neurosci* **12**: 6.

1084 Sur, M. and J. L. Rubenstein (2005). "Patterning and plasticity of the cerebral cortex." *Science*
1085 **310**(5749): 805-810.

1086 Sutcliffe, B., M. G. Forero, B. Zhu, I. M. Robinson and A. Hidalgo (2013). "Neuron-type specific
1087 functions of DNT1, DNT2 and Spz at the Drosophila neuromuscular junction." *PLoS One* **8**(10):
1088 e75902.

1089 Talay, M., E. B. Richman, N. J. Snell, G. G. Hartmann, J. D. Fisher, A. Sorkac, J. F. Santoyo, C. Chou-
1090 Freed, N. Nair, M. Johnson, J. R. Szymanski and G. Barnea (2017). "Transsynaptic Mapping of Second-
1091 Order Taste Neurons in Flies by trans-Tango." *Neuron* **96**(4): 783-795 e784.

1092 Tamada, M., J. Shi, K. S. Bourdot, S. Supriyatno, K. H. Palmquist, O. L. Gutierrez-Ruiz and J. A. Zallen
1093 (2021). "Toll receptors remodel epithelia by directing planar-polarized Src and PI3K activity." *Dev*
1094 *Cell* **56**(11): 1589-1602 e1589.

1095 Tauszig, S., E. Jouanguy, J. A. Hoffmann and J. L. Imler (2000). "Toll-related receptors and the control
1096 of antimicrobial peptide expression in Drosophila." *Proc Natl Acad Sci U S A* **97**(19): 10520-10525.

1097 Technau, G. M. (1984). "Fiber number in the mushroom bodies of adult Drosophila melanogaster
1098 depends on age, sex and experience." *J Neurogenet* **1**(2): 113-126.

1099 Tessarollo, L. and S. Yanpallewar (2022). "TrkB Truncated Isoform Receptors as Transducers and
1100 Determinants of BDNF Functions." *Front Neurosci* **16**: 847572.

1101 Ulian-Benitez, S., S. Bishop, I. Foldi, J. Wentzell, C. Okenwa, M. G. Forero, B. Zhu, M. Moreira, M.
1102 Phizacklea, G. McIlroy, G. Li, N. J. Gay and A. Hidalgo (2017). "Kek-6: A truncated-Trk-like receptor
1103 for Drosophila neurotrophin 2 regulates structural synaptic plasticity." *PLoS Genet* **13**(8): e1006968.

1104 Vahid-Ansari, F. and P. R. Albert (2021). "Rewiring of the Serotonin System in Major Depression."
1105 *Front Psychiatry* **12**: 802581.

1106 Vaughen, J. P., E. Theisen, I. M. Rivas-Serna, A. B. Berger, P. Kalakuntla, I. Anreiter, V. C. Mazurak, T.
1107 P. Rodriguez, J. D. Mast, T. Hartl, E. O. Perlstein, R. J. Reimer, M. T. Clandinin and T. R. Clandinin
1108 (2022). "Glial control of sphingolipid levels sculpts diurnal remodeling in a circadian circuit." *Neuron*
1109 **110**(19): 3186-3205 e3187.

1110 Waddell, S. (2013). "Reinforcement signalling in Drosophila; dopamine does it all after all." *Curr Opin*
1111 *Neurobiol* **23**(3): 324-329.

1112 Wang, C. S., E. T. Kavalali and L. M. Monteggia (2022). "BDNF signaling in context: From synaptic
1113 regulation to psychiatric disorders." *Cell* **185**(1): 62-76.

1114 Ward, A., W. Hong, V. Favaloro and L. Luo (2015). "Toll receptors instruct axon and dendrite
1115 targeting and participate in synaptic partner matching in a Drosophila olfactory circuit." *Neuron*
1116 **85**(5): 1013-1028.

1117 Weber, A. N., S. Tauszig-Delamasure, J. A. Hoffmann, E. Lelievre, H. Gascan, K. P. Ray, M. A. Morse,
1118 J. L. Imler and N. J. Gay (2003). "Binding of the Drosophila cytokine Spatzle to Toll is direct and
1119 establishes signaling." *Nat Immunol* **4**(8): 794-800.

1120 Wiesel, T. N. (1982). "Postnatal development of the visual cortex and the influence of environment."
1121 *Nature* **299**(5884): 583-591.

1122 Wohleb, E. S., T. Franklin, M. Iwata and R. S. Duman (2016). "Integrating neuroimmune systems in
1123 the neurobiology of depression." *Nat Rev Neurosci* **17**(8): 497-511.

1124 Woollett, K. and E. A. Maguire (2011). "Acquiring "the Knowledge" of London's layout drives
1125 structural brain changes." *Curr Biol* **21**(24): 2109-2114.

1126 Yacoubian, T. A. and D. C. Lo (2000). "Truncated and full-length TrkB receptors regulate distinct
1127 modes of dendritic growth." *Nat Neurosci* **3**(4): 342-349.

1128 Yang, T., Z. Nie, H. Shu, Y. Kuang, X. Chen, J. Cheng, S. Yu and H. Liu (2020). "The Role of BDNF on
1129 Neural Plasticity in Depression." *Front Cell Neurosci* **14**: 82.

1130 Zhang, J., T. Tang, R. Zhang, L. Wen, X. Deng, X. Xu, W. Yang, F. Jin, Y. Cao, Y. Lu and X. Q. Yu (2024).
1131 "Maintaining Toll signaling in Drosophila brain is required to sustain autophagy for dopamine
1132 neuron survival." *iScience* **27**(2): 108795.

1133 Zhu, B., J. A. Pennack, P. McQuilton, M. G. Forero, K. Mizuguchi, B. Sutcliffe, C. J. Gu, J. C. Fenton
1134 and A. Hidalgo (2008). "Drosophila neurotrophins reveal a common mechanism for nervous system
1135 formation." *PLoS Biol* **6**(11): e284.
1136

1137

1138 FIGURE LEGENDS

1139 **Figure 1 Neurons expressing *DNT-2* and its receptors *Toll-6* and *kek-6* in the adult brain**

1140 **(A)** *DNT-2A* expressing neurons (*DNT-2>FlyBow1.1* in green; anti-Brp in magenta) have cell bodies in SOG
1141 and project to FLA/PRW and SMP. **(B,D)** Pre-synaptic (green) and post-synaptic (magenta) terminals of
1142 DNT-2A neurons seen with *DNT-2>DenMark::RFP, Dsyd1::GFP*, higher magnification in **(D),** different
1143 specimens from (B). DNT-2A projections at SMP and PRW have both pre- and post-synaptic sites. **(C)** Single
1144 neuron DNT-2A>MCFO clones. **(E)** Left: DNT-2A neurons have the vesicular glutamate transporter vGlut
1145 (arrows). Right: Colocalization between *Dop2RLex>AopCD8-GFP* and *DNT2Gal4>UASCD8-RFP* in cell bodies
1146 of DNT-2A neurons (arrows). **(F)** Terminals of dopaminergic neurons (*TH>mCD8GFP*) abut and overlap those
1147 of DNT-2A neurons (*DNT2>CD8-RFP*, magenta), arrows; magnified projections on the right. **(G)** Illustration
1148 of neurons expressing DNT-2 (magenta) and KCs, DAN PAM and PPL1, and DAL neurons **(H)** *Toll-*
1149 *6>FlyBow1.1* is expressed in Kenyon cells, PPL1, PPL2 and PAM DANs, as revealed by co-localization with
1150 anti-TH. **(I)** *kek-6>FlyBow1.1* co-localises with TH in MB vertical lobes, dopaminergic PALs, VUMs, PPL1,
1151 PPM2 and PPM3. SMP: superior medial protocerebrum, PRW: Prow, FLA: Flange, SOG: sub-aesophageal
1152 ganglion. Scale bars: (A-C, F-left, H, I) 50µm; (D,E,F-right) 25µm.

1153

1154 **Figure 2 DNT-2 neurons are functionally connected to dopaminergic neurons**

1155 **(A)** TransTango revealed out-puts of DNT-2 neurons. All neurons express *TransTango* and expression of the
1156 TransTango ligand in DNT-2 neurons identified DNT-2 out-puts with Tomato (anti-DsRed). TransTango
1157 identified as DNT-2 outputs KC $\alpha'\beta'$ MB lobes (anterior brain, arrow, **top left**); Kenyon and possibly DAN cell
1158 bodies (posterior, arrows **top right**); DAL neurons **(bottom left,** arrows) and the dorsal layer of the fan
1159 shaped body **(bottom right,** arrow). See also Supplementary Figure S3 for further controls. **(B)** BAcTrace

1160 tests connectivity to a candidate neuron input visualised with *LexAop>sybGFP* by driving the expression of a
1161 ligand from *DNT-2GAL4* that will activate *QUASTomato* in the candidate input neuron (Cachero et al. 2020).
1162 Candidate PAM neurons visualised at SMP with GFP (green): Control: *R58E02LexA>BAcTrace 806*, no *GAL4*.
1163 Test: *R58E02LexA, DNT-2GAL4>BAcTrace 806* revealed PAMs are inputs of DNT-2A neurons at SMP
1164 (Tomato, bottom). Magenta shows QUAS-Tomato. **(C)** qRT-PCR showing that TH mRNA levels increased
1165 with DNT-2 over-expression at 30°C *(tubGAL80^{ts}, DNT-2>DNT-2FL).* One way ANOVA, P=0.0085; post-doc
1166 Dunnett's multiple comparison test**. (D)** FRET cAMP probe Epac1 revealed that *DNT-2>Dop2R-RNAi*
1167 knockdown decreased YFP/CFP ratio over time in DNT-2A neurons, meaning that cAMP levels increased.
1168 Two-way ANOVA, genotype factor p<0.0001, time factor p<0.0001; post-doc Dunnett's. **(E,F)** Summary:
1169 DNT-2 neurons and DANs are functionally connected and modulate each other. **(E)** DNT-2 can induce *TH*
1170 expression in DANs; **(F)** this is followed by negative feedback from DANs to DNT-2 neurons. TH: tyrosine
1171 hydroxylase. Scale bars: (A) 50µm; (B) 30µm; (D) 20µm. P values over graphs in (C) refer to group analyses;
1172 stars indicate multiple comparisons tests. *p<0.05,**p<0.01, ***p<0.001. For sample sizes and further
1173 statistical details, see Supplementary Table S2.
1174
1175 **Figure 3 DNT-2 and Toll-6 maintain PAM neuron survival in the developing and adult brain.**
1176 **(A)** Illustration of PAM neuronal cell bodies and experimental temporal profile. DANs are shown in green,
1177 DNT-2A neurons in magenta and MB in dark grey. The left hemisphere shows the anterior brain with PAL
1178 and PAM DAN neurons (green) and DNT-2 neurons (magenta); the right shows the posterior brain, with the
1179 calyx and other DAN neurons (PPM1, PPM2, PPM3, PPL1, PPL2, green). **(B-D)** Fruit-flies were kept
1180 constantly at 25°C, from development to adult. Analyses done in adult brains**. (B)** *DNT-2^{37}/DNT-2^{18}* mutants
1181 had fewer histone-YFP+ labelled PAM neurons (*THGAL4, R58E02-GAL4>hisYFP).* Un-paired Student t-test.
1182 **(C)** *Toll-6* RNAi knock-down in all DANs (*THGAL4, R58E02-GAL4>hisYFP, Toll-6 RNAi)* reduced Histone-YFP+
1183 labelled PAM cell number. Un-paired Student t-test. **(D)** *DNT-2^{37}/DNT-2^{18}* mutants had fewer PAMs stained
1184 with anti-TH antibodies. Over-expressing *Toll-6^{CY}* in DANs (*THGAL4, R58E02 GAL4>hisYFP, Toll-6^{CY}*) rescued
1185 TH+ PAM neurons in *DNT-2^{37}/DNT-2^{18}* mutants, demonstrating that DNT-2 functions via Toll-6 to maintain

1186 PAM cell survival. Welch ANOVA p<0.0001, post-hoc Dunnett test. **(E-H)** Adult specific restricted over-
1187 expression or knock-down at 30°C, using the temperature sensitive GAL4 repressor *tubGAL80^{ts}*. **(E)** Adult
1188 specific *DNT-2* RNAi knockdown in DNT-2 neurons decreased Tomato+ PAM cell number (*tubGAL80^{ts},*
1189 *R58E02-LexA, DNT-2 GAL4>LexAOP-Tomato, UAS DNT-2-RNAi*). Un-paired Student t-test, p= 0.005. **(F)** Adult
1190 specific *Toll-6* RNAi knock-down in *Toll-6^{31}* heterozygous mutant flies in DANs, reduced Histone-YFP+ PAM
1191 cell number (*tubGAL80^{ts}; THGAL4, R58E02-GAL4>hisYFP, Toll-6 RNAi/Toll6^{31}*). Un-paired Student t-test. **(G)**
1192 PAMs were visualised with anti-TH. Left: *tubGAL80^{ts}, Toll-6>Toll-6-RNAi* knock-down decreased TH+ PAM
1193 cell number. Un-paired Student t-test. Right: *tubGAL80^{ts}, DNT-2>DNT-2-RNAi* knock-down decreased TH+
1194 PAM cell number. Kruskal-Wallis ANOVA, p=0.0001, post-hoc Dunn's test. **(H)** Adult-specific *tubGAL80^{ts},*
1195 *DNT-2>DNT-2RNAi* knock-down increased the number of apoptotic cells in the brain labelled with anti-DCP-
1196 1. Dcp-1+ cells co-localise with anti-TH at least in PAM clusters. One Way ANOVA, p<0.0001, post-doc
1197 Bonferroni's multiple comparisons test. DANs>histone-YFP: all dopaminergic neurons expressing histone-
1198 YFP, genotype: *THGal4 R58E02Gal4>UAS-histoneYFP*. *PAMsLexA>tomato*: restricted to PAM DANs:
1199 *R58E02LexA>LexAop-nlstdTomato.* Controls: *GAL4* drivers crossed to wild-type Canton-S. Scale bars: (B-G)
1200 30µm; (H) 20µm. Graphs show box-plots around the median. P values over graphs in (D, G right, H) refer to
1201 group analyses; stars indicate multiple comparisons tests. *p<0.05, **p<0.01, ***p<0.001. For further
1202 genotypes, sample sizes and statistical details, see Supplementary Table S2.
1203
1204 **Figure 4 DNT-2, Toll-6 and Kek-6 are required for arborisations and synapse formation. (A)**
1205 Illustration showing the ROIs (dashed lines) used for the analyses, corresponding to dendrites and axonal
1206 endings of PAMs and axonal terminals of PPL1ped neurons. **(B-F)** Fruit-flies were kept constantly at 25°C.
1207 **(B)** Complete loss of PAM synapses (*PAM>syt-GFP*) onto α,β MB lobe in *DNT-2* null mutants. **(C)** *Toll-6* RNAi
1208 knockdown in PAM β2β'2 neurons (*MB301B>FB1.1, Toll-6-RNAi*) decreased dendrite complexity. Un-paired
1209 Student t-test. **(D)** Over-expression of cleaved *DNT-2CK* in PAM β2β'2 neurons *(MB301B>CD8-GFP, DNT-*
1210 *2CK)* increased dendrite complexity. Un-paired Student t-test. **(E,E',F)** PPL1ped axonal misrouting was
1211 visualised with *split-GAL4 MB320CGal4>FlyBow1.1.* Images show PPL1-γped neurons and some PPL1-

1212 α2α'2. **(D,D')** RNAi knock-down of *Toll-6, kek-6* or both (e.g. *MB320CGal4>FlyBow1.1, Toll-6RNAi)* in PPL1-
1213 γped neurons caused axonal terminal misrouting (arrows). **(E')** Higher magnification of **(E,** dotted squares**)**.
1214 Chi-square for group analysis: p = 0.0224, and multiple comparisons Bonferroni correction control vs *Toll-*
1215 *6RNAi* p<0.01; vs *kek-6RNAi* p<0.05; vs *Toll-6RNAi kek-6RNAi* p<0.01, see Table S2**. (F)** PPL1 misrouting was
1216 also induced by over-expressed *DNT-2CK* or *DNT-2FL* (e.g. *MB320CGal4>FlyBow1.1, DNT-2FL)*. Chi-square
1217 for group analysis: p<0.05, Bonferroni correction control vs *DNT-2CK* ns, vs *DNT-2FL* *p<0.05, see Table S2.
1218 **(G)** Adult-specific *Toll-6 kek-6 RNAi* knockdown in PAM neurons decreased size of post-synaptic density
1219 sites (*PAM>Homer-GCaMP* and anti-GFP antibodies). Temperature regime shown on the right. **(C,D)** Graphs
1220 show box-plots around the median; **(G)** are box-plots with dot plots. (C,D,G) *p<0.05, **p<0.01,
1221 ****p<0.0001. Scale bars: (B,C,D,E) 30µm; (E',F,G) 20µm. For genotypes, sample sizes and statistical details,
1222 see Supplementary Table S2.
1223
1224 **Figure 5 DNT-2 neuron activation and DNT-2 over-expression induced synaptogenesis. (A)**
1225 Thermo-activation of DNT-2 neurons at 30°C altered DNT-2 arborisations, here showing an example with
1226 smaller dendrites and enlarged axonal arbours (magenta shows 3D-rendering of axonal arborisation done
1227 with Imaris, merged with raw image in green). (Genotype: *DNT-2>FlyBow1.1, TrpA1*). **(B)** Thermogenetic
1228 activation of DNT-2 neurons increased the number of Homer+ PSDs in DNT-2 neurons, at SMP (*DNT-*
1229 *2>Homer-GCAMP3, TrpA1*, anti-GFP). Test at 30°C 24h: Unpaired Student t test. See Table S2. **(C)**
1230 Thermogenetic activation of DNT-2 neurons induced synaptogenesis in PAM target neurons at SMP, but not
1231 at MB lobe. (Genotype: *PAM(R58E02)LexA/LexAOP-sytGCaMP; DNT-2GAL4/UASTrpA1*). At SMP: No. Syt+
1232 synapses: Mann Whitney-U; Syt+ synapse volume: Mann Whitney-U. At MB lobe: No. Syt+ synapses:
1233 Unpaired Student t ns; Syt+ synapse volume: Mann Whitney-U ns. **(D)** Over-expression of DNT-2FL in DNT-
1234 2 neurons increased synapse volume at SMP dendrite and induced synaptogenesis at MB lobe. (Genotype:
1235 *PAM(R58E02)LexA/LexAopSytGcaMP6; DNT-2Gal4/UAS-DNT-2FL*). At SMP: No. Syt+ synapses: Unpaired
1236 Student t ns. Syt+ synapse volume: Mann Whitney-U. At MB lobe: No. Syt+ synapses: Unpaired Student t;
1237 Syt+ synapse volume: Mann Whitney-U ns. Graphs show box-plots around the median, except for PSD

1238 volume data that are dot plots. *p<0.05, ****p<0.0001; ns: not significantly different from control. Scale
1239 bars: 30µm. For Genotypes, sample sizes, p values and other statistical details, see Supplementary Table S2.
1240
1241 **Figure 6 DNT-2-induced circuit plasticity modified dopamine-dependent behaviour. (A)** *DNT-2*
1242 mutants (left, *DNT-2^{37}/DNT-2^{18}*) and flies with adult-specific RNAi knock-down of *DNT-2* in DNT-2 neurons
1243 (right, *tubGAL80^{ts}; DNT-2>DNT-2RNAi*), had impaired climbing. Left Mann Whitney U; Right: One Way
1244 ANOV, post-hoc Dunnett. **(B)** Adult-specific *Toll-6* and *kek-6* RNAi knock-down in Toll-6 *(tubGAL80^{ts}; Toll-*
1245 *6>Toll-6RNAi, kek-6RNAi,* left) or PAM (*tubGAL80^{ts}; R58E02>Toll-6RNAi, kek-6RNAi,* right) neurons impaired
1246 climbing. Left: Welch ANOVA, post-hoc Dunnett. Right: Welch ANOVA, post-hoc Dunnett. **(C)** The climbing
1247 impairment of *DNT-2* mutants could be rescued with the over-expression of *Toll-6^{CY}* in dopaminergic
1248 neurons (Rescue genotype: UASToll-6^{CY}/+; DNT-2^{18}*THGAL4 R58E02GAL4/DNT-2^{37}).* Welch ANOVA, post-hoc
1249 Dunnett. **(D)** Adult specific over-expression of *Toll-6^{CY}* in DANs increased locomotion in *DNT-2^{37}/DNT-2^{18}*
1250 mutants. (Test genotype: *UASToll-6^{CY}/+; DNT-2^{18}THGAL4 R58E02GAL4/DNT-2^{37}*). Walking speed: Kruskal
1251 Wallis ANOVA, post-hoc Dunn's. Distance walked: Kruskal Wallis ANOVA, post-hoc Dunn's. Time spent
1252 immobile: Kruskal Wallis ANOVA, post-hoc Dunn's. **(E)** Adult specific *DNT-2FL* overexpression in DNT-2
1253 neurons increased fruit-fly locomotion speed in an open arena at 30°C (see also Supplementary Figure S6A
1254 for further controls). (Test genotype: *tubGAL80^{ts}, DNT-2>DNT-2FL*) Kruskal-Wallis, post-hoc Dunn's test. **(F)**
1255 Thermogenetic activation of DNT-2 neurons at 30°C *(DNT-2>TrpA1)* increased fruit-fly locomotion speed.
1256 (See also Supplementary Figure S6B for further controls). One Way ANOVA p<0.0001, post-hoc Dunnett's
1257 test**. (G)** Over-expression of *DNT-2-FL* in DNT-2 neurons increased long-term memory. (Test genotype:
1258 *tubGAL80^{ts}, DNT-2>DNT-2FL*). Left: 23°C controls: One Way ANOVA p=0.8006. Right 30°C: One Way ANOVA,
1259 post-hoc Dunnett's test. Graphs show box-plots around the median, under also dot plots. P values over
1260 graphs refer to group analyses; asterisks indicate multiple comparisons tests. *p<0.05, **p<0.01,
1261 ***p<0.001, ****p<0.0001; ns: not significantly different from control. For further genotypes, sample sizes,
1262 p values and other statistical details, see Supplementary Table S2.
1263

1264 SUPPLEMENTAL INFORMATION

1265 **Supplementary Figure S1 Identification of neurotransmitter type for DNT-2A neurons. (A, B)**
1266 Anterior DNT-2A neurons projecting at SMP are not dopaminergic, as there was no co-localisation between
1267 *DNT-2>histoneYFP* and anti-TH in the anterior brain **(A),** and there was no colocalization in other DNT-2+
1268 neurons in the posterior brain either **(B).** Higher magnification of dotted boxes on the right. **(C)** There was
1269 no colocalisation with *Dop1R2LexA>CD8::GFP, DNT-2Gal4>CD8::RFP* either. **(D)** DNT-2 neurons are not not
1270 serotonergic, as there was no co-localization between *DNT-2>FlyBow1.1* and the serotoninergic neuron
1271 marker anti-5HT**. (E)** There are not octopaminergic, as there was no overlap between *TdcLexA>mCD8::GFP*
1272 *and DNT-2Gal4>CD8::RFP*. **(F)** There was no overlap between *DNT-2Gal4>histoneYFP* and the cholinergic
1273 neuron marker anti-ChAT4b1. **(G,H)** Anterior DNT-2A neurons are not GABAergic, but lateral DNT-2 neurons
1274 are, as visualised with *DNT-2>CD8-RFP, GADLexA>CD8-GFP*. Scale bars: (A,B left) 50µm; (C-H) 20 µm. For
1275 further genotypes and sample sizes, see Supplementary Table S2.

1276

1277 **Supplementary Figure S2 Identification of *Toll-6* and *kek-6* expressing neurons. (A)** *Toll-6Gal4,*
1278 *MB247-Gal80>UASFlyBow1.1* and *kek-6Gal4, MB247-Gal80>UASFlyBow1.1* revealed Toll-6+ and Kek-6+
1279 projections on MB g2a'1. **(B)** *R25D01LexA>CD8GFP, kek6-Gal4>CD8RFP* overlapped in MB g2a'1. **(C)**
1280 *R14C08LexA>CD8GFP, Toll-6Gal4>CD8-RFP13* revealed co-localization in MBON-M4/M6 cell bodies. **(D,E)**
1281 Co-localisation of *Toll-6>Histone-YFP* and *kek-6>HistoneYFP* with TH in PPL1 neurons. **(F)** Number of PAM
1282 and PPL1 neurons expressing *Tolls* and *kek-6,* revealed from published RNAseq data (Scope, see also Table
1283 S1). **(G, H)** Toll-6 and kek-6 are expressed in DAL neurons. **(G)** DAL neurons express *Toll-6,* as revealed by
1284 co-localization between *DAL-LexA (VT49239-LexA)>mCD8-GFP* and *Toll-6GAL4>mCD8-RFP*. **(H)** DAL neurons
1285 express *kek-6*, as revealed by colocalization between *DAL-LexA (VT49239-LexA)>mCD8-GFP* and
1286 *kek6GAL4>mCD8RFP*. **(I, J)** Toll-6 and kek-6 are expressed in MB neurons. **(I)** *Toll-6>MCFO* clones reveal
1287 expression at least in MB neurons g medial (gm), abcore (abc) and absurface (abs). **(K)** *kek-6>MCFO* clones
1288 reveal expression at least in MB Kenyon cells aba'b'g formed and MB g2a'1 and a2a'2 and PPL1-$\gamma 2\alpha'1$ and

1289 PPL1-α2α'2. Scale bars: (B, H) 50µm; (A,C,D,G, I, J) 30µm. For further genotypes and sample sizes, see
1290 Supplementary Table S2.
1291
1292 **Supplementary Figure S3 TransTango connectivity controls. (A)** *UAS-TransTango/+* control, showing
1293 background GFP expression in mushroom bodies and Tomato+ signal in sub-aesophageal ganglion (SOG).
1294 **(B)** *DNT-2GAL4>UAS-TransTango*, revealing the GFP+ DNT-2 neurons and Tomato+ signal in DNT-2 neurons.
1295 TransTango also reveals what appears to be feedback connections between DNT-2 neurons from SMP to
1296 PRW (arrow). These are controls for Figure 3A. Scale bars: (A,B) 50µm. For further genotypes and sample
1297 sizes, see Supplementary Table S2.
1298
1299 **Supplementary Figure S4 Neuronal activity increased production and cleavage of DNT-2. (A)**
1300 Thermogenetic activation of DNT-2 neurons increased the number of DNT-2FLGFP+ vesicles or spots (*DNT-*
1301 *2>DNT-2-FL-GFP*, *TrpA1* with anti-GFP). Control 18°C: Unpaired Student t test, ns. Activation 30°C 24h:
1302 Mann Whitney**. (B)** Western blot from fly heads over-expressing DNT-2FL-GFP in DNT-2 neurons showing
1303 that neuronal activation with TrpA1 at 30°C increased DNT-2FL-GFP cleavage. **(**Genotype: *DNT-2>TrpA1,*
1304 *DNT-2FL-GFP*). Controls are flies of the same genotype kept constantly at 18°C as well as flies treated also
1305 at 30°C but lacking TrpA1. High temperature (30°C) is sufficient to increase fly activity. ***p<0.001. ns= not
1306 significant. For further genotypes, sample sizes, p values and other statistical details see Supplementary
1307 Table S2.
1308
1309 **Supplementary Figure S5 Controls for Figure 5B.** Control at 18°C, for Figure 5B. DNT-2 bidirectional
1310 arborisation at SMP was visualised with Homer-GCaMP and anti-GFP antibodies (*DNT-21>homer-GCAMP*
1311 and *DNT-2>homer-GCAMP, TrpA1* at 18°C). Unpaired Student t-test, ns. Scale bars: (A,B) 30µm. For further
1312 genotypes, sample sizes, p values and other statistical details see Supplementary Table S2.
1313

1314 **Supplementary Figure S6** **Locomotion in open arena controls. (A)** Controls for Figure 6E. In 18°C
1315 controls, GAL80 is on and GAL4 is off, thus there is no adult specific *DNT-2FL* overexpression in DNT-2
1316 neurons in these flies. (Genotype: *tubGAL80ts, DNT-2>DNT-2FL*). Consistently, there was no increase in
1317 locomotion speed in an open arena, in flies over-expressing *DNT-2FL* relative to controls, compare also to
1318 Figure 6E. Kruskal Wallis ANOVA ns (lower median in *UAS-DNT-2FL/+* control). **(B)** Controls for Figure 6F.
1319 The cation TrpA1 opens at high temperatures (eg 30°C) but remains closed at 18°C. Consistently, there was
1320 no effect in locomotion at 18°C in flies of genotype *DNT-2>TrpA1* compared to controls, compare also to
1321 30°C data in Figure 6F. Kruskal Wallis ANOVA ns. For further genotypes, sample sizes, p values and other
1322 statistical details see Supplementary Table S2.
1323
1324 **Supplementary Figure S7** **Altering *DNT-2* levels induced seizures.** Knock-down or over-expression of
1325 *DNT-2* in the adult, using $GAL80^{ts}$. Fruit-flies were reared at 18°C from egg laying to adult eclosion, when
1326 they were transferred to 30°C and kept there for 5 days prior to testing**.** To test for seizures, we used the
1327 bang-sensitivity test. $DNT2^{37}/DNT2^{18}$ mutant flies (left) and adult *DNT-2* knock-down flies ($tubGal80^{ts}$ *DNT-*
1328 *2Gal4>DNT-2RNAi,* centre) took longer to recover than controls. Over-expression of *DNT-2FL* in DNT-2
1329 neurons ($tubGal80^{ts}$ *DNT-2Gal4>DNT-2FL,* right) increased variability in recovery time. For further
1330 genotypes and sample sizes see Supplementary Table S2.
1331
1332 **Table S1** **Expression of *Tolls, keks* and Toll downstream adaptors in cells related to DNT-2A**
1333 **neurons.** Genes expressed in DNT-2 neurons, their potential and/or experimentally verified inputs and
1334 outputs, were identified with a combination of reporters (this work) and data from public single-cell
1335 RNAseq databases.
1336
1337 **Table S2** **Statistical analysis.** Table providing full genotypes, sample sizes, statistical tests, multiple
1338 comparison corrections and p values.
1339

FIGURE 1 Neurons expressing *DNT-2* and its receptors *Toll-6* and *kek-6* in the adult brain

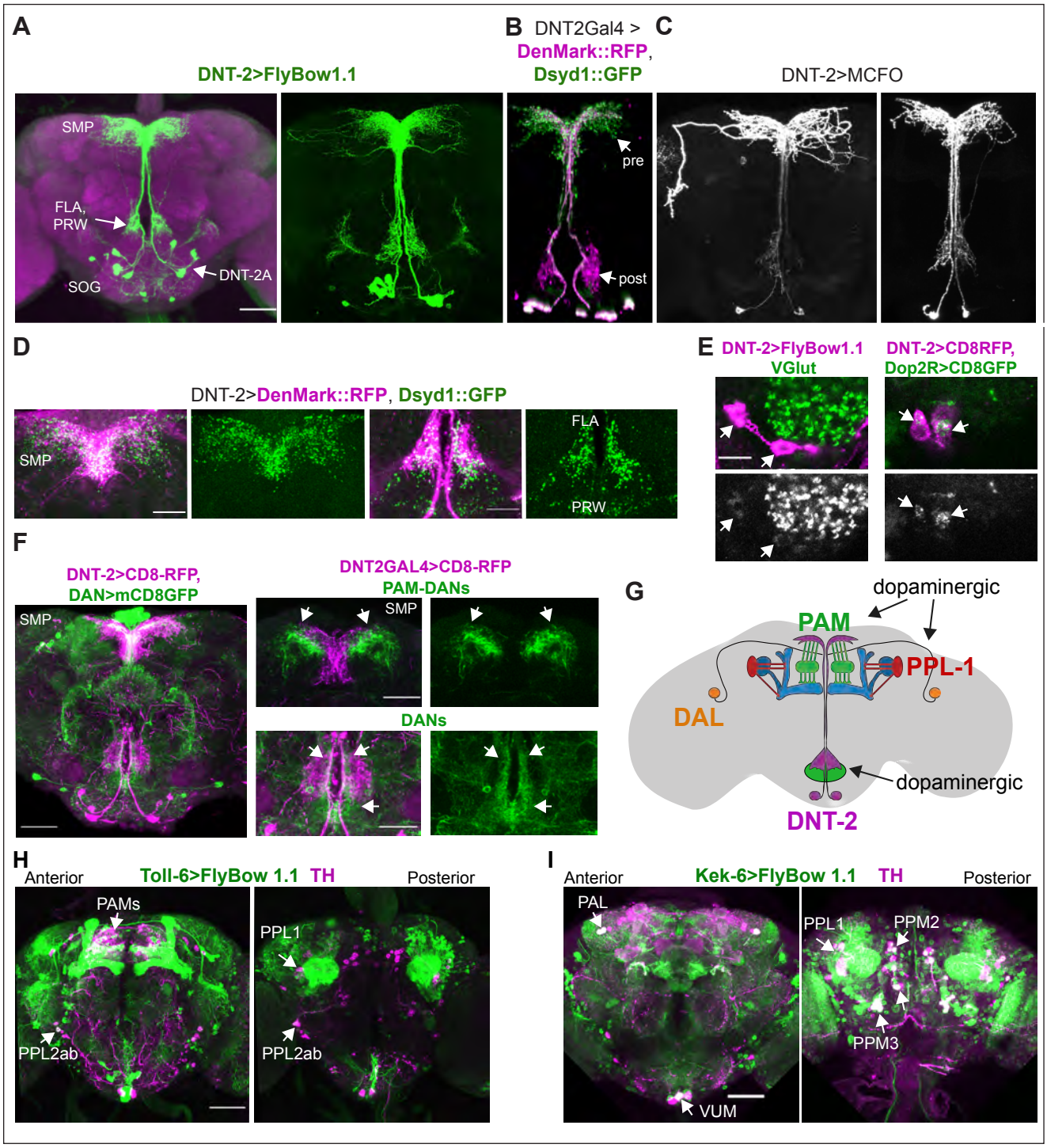

Figure 2 DNT-2 neurons are functionally connected to dopaminergic neurons

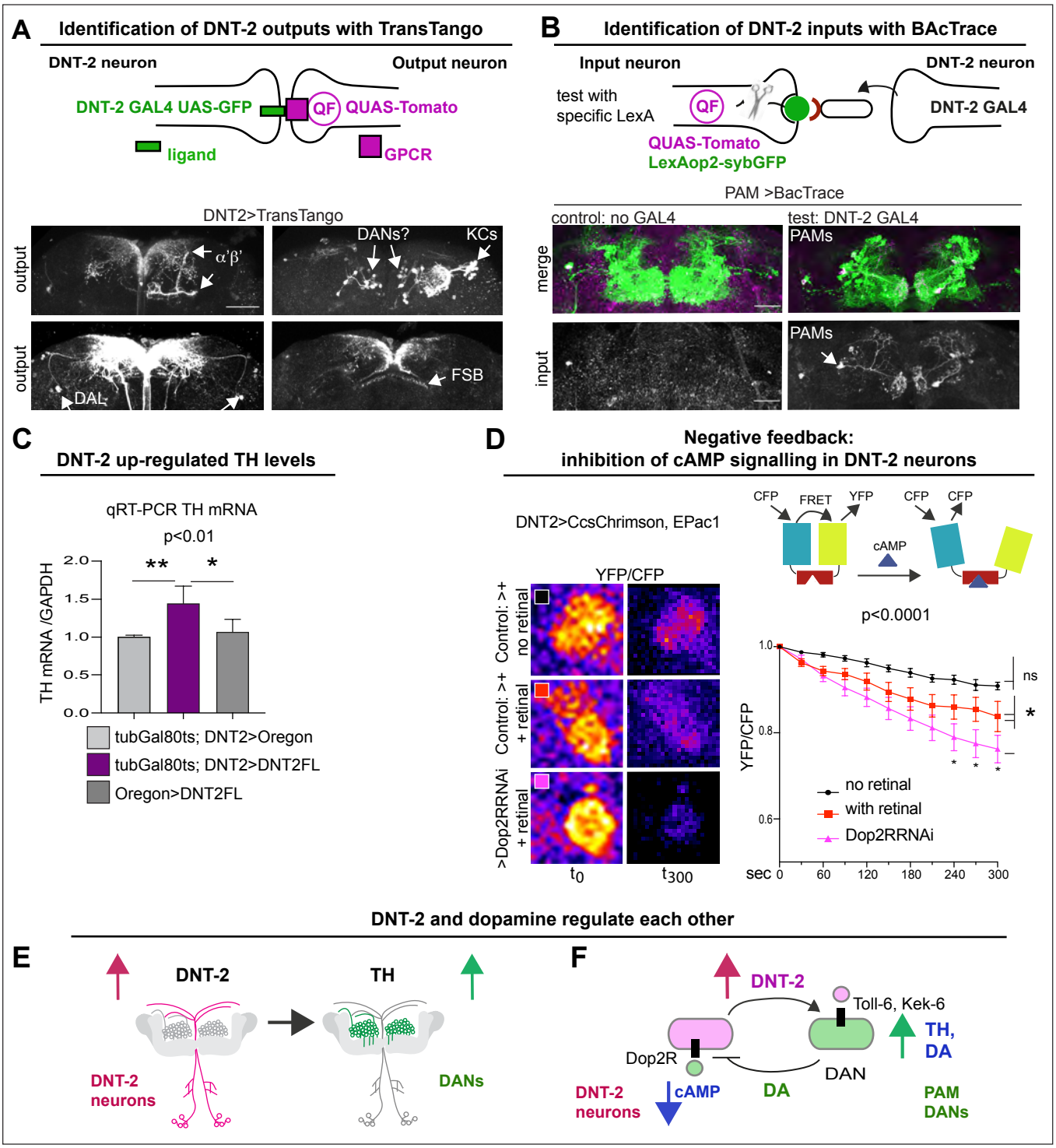

Figure 3 DNT-2 and Toll-6 maintain PAM neuron survival in the developing and adult brain

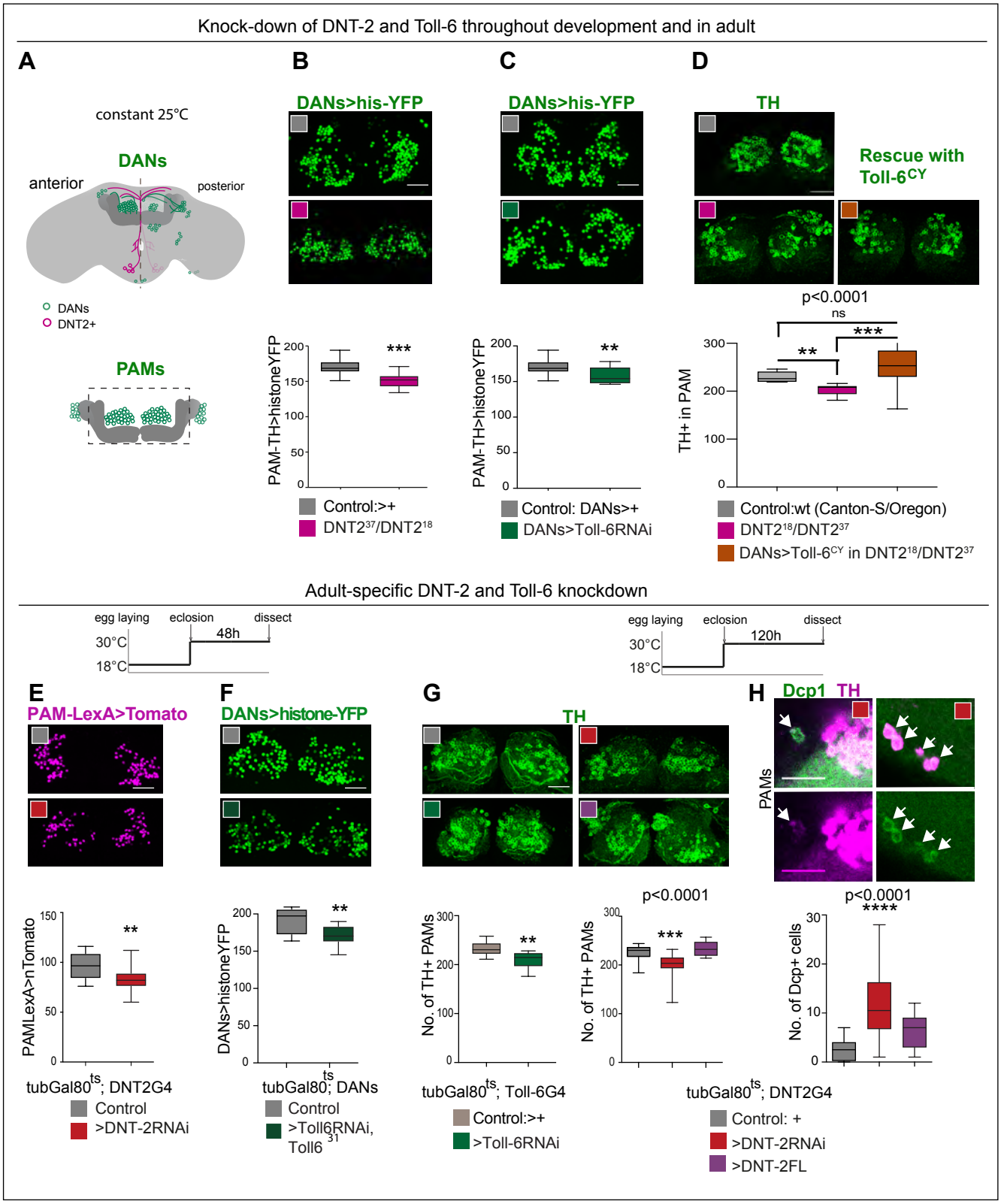

Figure 4 DNT-2, Toll-6 and Kek-6 are required for synapse formation and arborisations

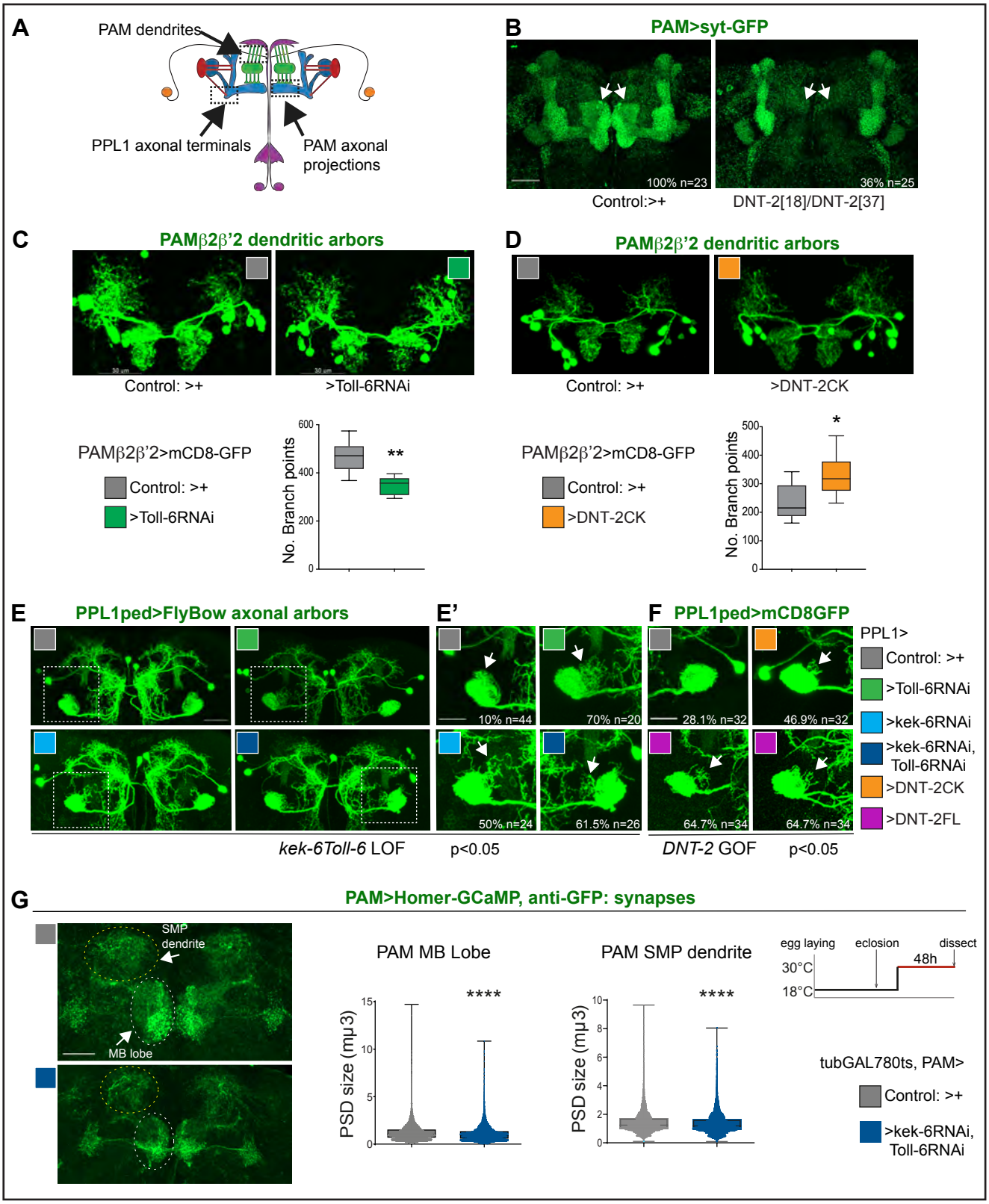

Figure 5 DNT-2 neuron activation and DNT-2 over-expression induce synaptogenesis

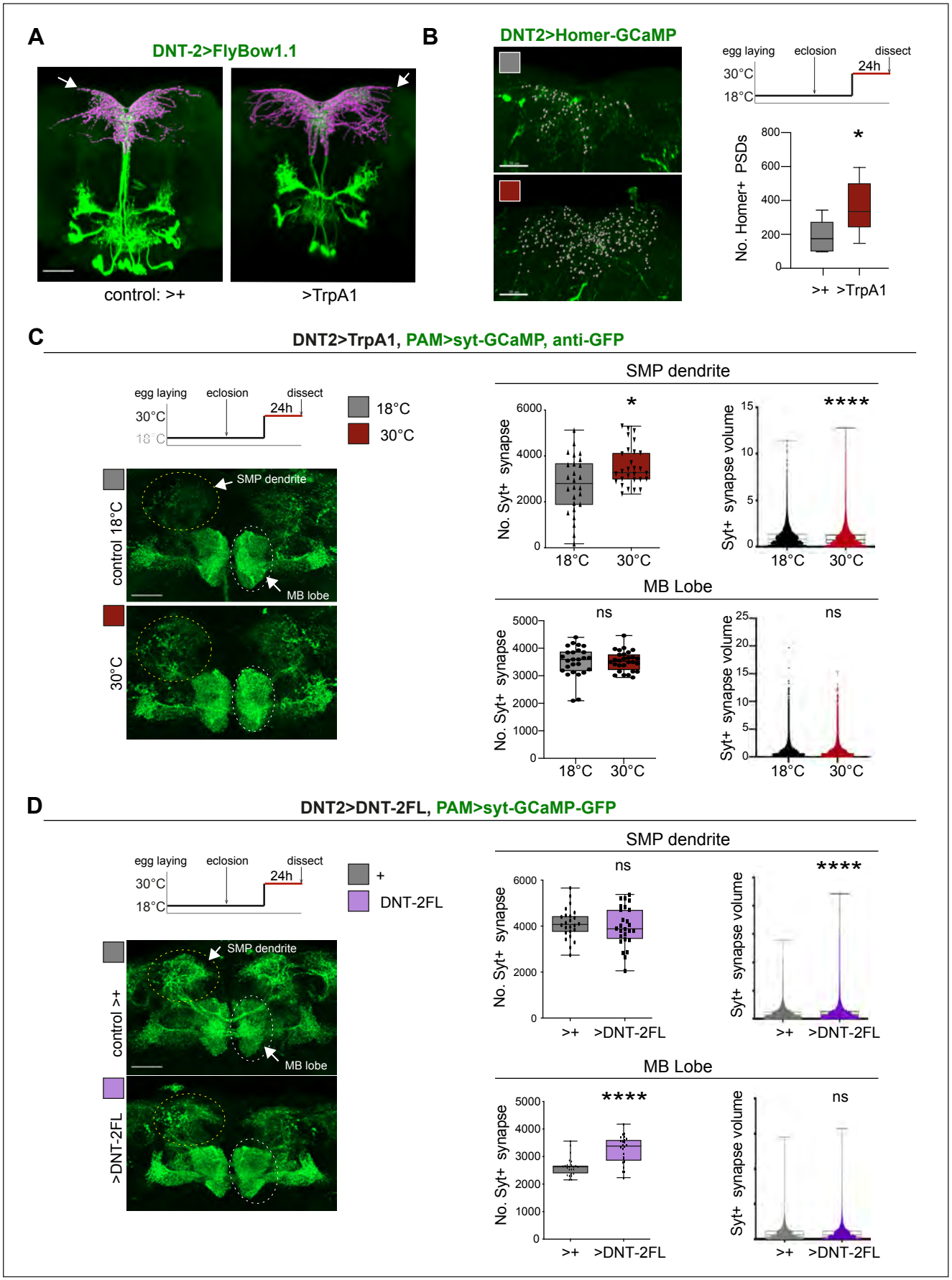
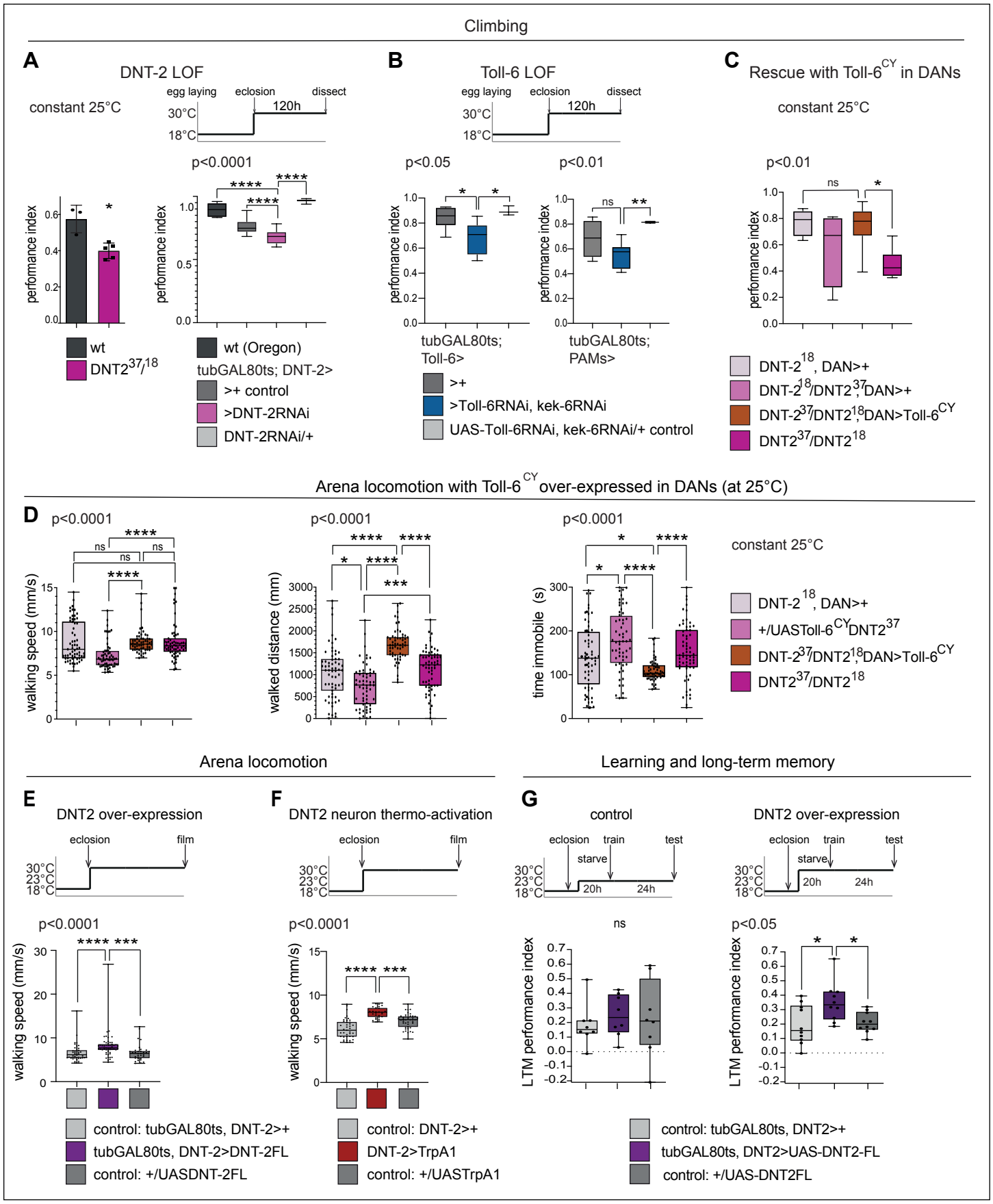
Figure 6 DNT-2-induced circuit plasticity modified dopamine-dependent behaviours.